POLITECNICO DI TORINO

Department of Electronics and Telecommunications

Master degree course in Communications and Computer Networks Engineering

Master Degree Thesis

Software-defined radio implementation of a video transmission system: a study of non-uniform digital constellations

Supervisors
Prof. Roberto Garello
Prof. Alberto Dassatti
Dr. Daniel G. Riviello

Candidate
Mahboob Karimian
Student No.: s246885

Academic year 2020-2021

To my dear mother, who is really a strong and kind woman.

Abstract

Emerging new wireless technologies and devices to capture and broadcast high–resolution videos in real–time, demand higher data transfer rates. To increase the bit rate, the communication systems always are under development. In the meantime, the other objective is low power consumption, especially for mobile devices like phones and cameras.
This achievement requires an optimum design of the elements in a transmission chain. One of the possibilities is optimizing the modulator block. Most of the standard communication systems like DVB—T, use the traditional uniform constellations to map multiple information bits to a constellation symbol. Optimizing the constellation leads to obtain "non–uniform" constellations.
In this work, we studied and designed the new "non–uniform" constellations which are used to close the capacity gap to the Shannon limit as much as possible. In this regard, we used the maximization of BICM capacity approach. BICM, which is a scheme to design a transmission chain and its blocks, tries to increase the code diversity, and because of its flexibility, the channel encoder and modulator can be chosen independently. This makes it a powerful tool to focus on the constellation in the modulator, without worrying about the impact of constellation optimization on the other blocks. By doing this, the improved constellations have a higher capacity which can be translated to gain in other terms like reduction in the power, or, lowering the Bit Error Rate (BER). However, this improvement is not without the cost. Non–uniform constellations will impose another level of complexity to the demodulation procedure in the receiver, because, in contrast to the uniform constellations, the modulation algorithm can not use the symmetry features that are present in the constellation shape. Fortunately, this problem is resolved by designing new methods to simplify the demapping procedure. Another issue is choosing the best performing constellation. Since the SNR factor is present in the channel capacity equation, we have a specific optimum constellation for each SNR value. Therefore, the target receivers and

operation parameters of the system must be selected carefully. Nevertheless, the performance evaluations showed the optimized constellations outperform the uniform one regardless of SNR.
To evaluate and verify the performance of resulting constellations, first, we used them in a simulation of a full transmission chain, and then, applied them to an SDR implementation of a video transmission system to observe the performance in a real system. The outcome of the evaluation proved the maximum power gain of 0.8 [dB].
One of the most interesting parts of this work is that, in general, thanks to the BICM approach and its flexibility, the new optimized constellations can be used in a wide range of applications and new technologies that are following that design scheme.

The real transmission chain used in this thesis is developed by the REDS Institute (HEIG–VD, Yverdon Les Bains, CH).
This thesis is organized in 2 parts:

- **Introduction:**
  Contains introduction, characteristics, and basics of operation of the model and system under study.

- **Optimization and Results:**
  Contains optimization procedures and algorithms, results analysis, and performance evaluation on a real system.

Acknowledgments

I would like to thank my supervisors Prof. Roberto Garello, Prof. Alberto Dassati, and Dr. Daniel G. Riviello for their guidance, support, and feedback.
Also, I want to express my gratitude to all who helped me and I benefited from their advice to resolve the challenges of this thesis. Some of them were my colleagues and friends in REDS Institute; Especially Sydney and Rick.
It is necessary to mention Ireen and Mathieu, who I lived in their apartment during my stay in Switzerland and we experienced very great moments together. Without their welcome and help, this adventure could be too challenging for me. I am also grateful to Mithra, my life partner. She helped me to revise this document both grammatically and technically.
Special thanks to Politecnico di Torino and HEIG–VD which provided all the facilities and resources to begin and finish my studies and this thesis.

Acronyms

1D–NUQAM One-dimensional non-uniform QAM.

APSK Amplitude and phase-shift keying.

AWGN Additive white Gaussian noise.

BC Coded modulation.

BER Bit-error rate.

BICM Bit-interleaved coded modulation.

BW bandwidth.

CR Code Rate.

DOF Degree of freedom.

FEC Forward Error Correction.

FFT Fast Fourier transform.

FPGA Field-programmable gate array.

LLR Log Likelihood Ratio.

LSB Least significant bit.

ML Maximum-Likelihood.

MSB Most significant bit.

NM Nelder–Mead optimization method.

NUC Non-uniform constellation.

OFDM Orthogonal frequency-division multiplexing.

PAPR peak-to-average power ratio.

PSK Phase-shift keying.

QAM Quadrature amplitude modulation.

QEF Quasi Error Free.

RS Reed-Solomon.

SDR Software-defined radio.

SER Sequence Error rate.

SNR Signal-to-noise ratio.

TCM Trellis-coded modulation.

TS Transport Stream.

Contents

List of Tables

List of Figures

Part I

Introduction

Chapter 1

Preface

1.1 DVB–T and REDS chain

ETSI developed several well-known standards for video and audio broadcasting. DVB–T and successor one, DVB–T2 are for the terrestrial TV and they are the most dominant and successful technologies comparing other standards like ATSC 3.

REDS institute used these standards to redesign the whole chain of the a transmitter and receiver, satisfying the specific project requirements. The resulting system contains a Reed-Solomon encoder cascaded by a Turbo encoder which helps to remove the inner-interleaver, comparing to traditional DVB–T architecture. This reduces the latency and increases the system performance. Another important change is moving towards the MIMO technology. Based on the description of the project, this is used to increase the bit-rate of the system to meet the project requirements. We will consider neither channel coding nor MIMO in this thesis. Instead, we are dealing with the other important elements of the chain: modulation constellations and corresponding demodulators. To further increase the performance of the system, one can think of shaping the constellation to reduce the gap from the Shannon capacity limit. Since the optimal distribution for an AWGN channel is Gaussian, we use the Geometry shaping method to make the transmitted signal to be closer to the Gaussian. This is called "Geometry shaping", because it is dealing with distances of the points in the constellation which is different from the other possibility, "Probability shaping". Probability shaping is very hard to apply to the signal as it tries to give Gaussian shape to the signal after FEC encoding and thus it must be reversed in the receiver [18].

1.2 State of the art

1.2.1 BICM systems

Coded Modulation (CM) is a system with the concatenation of an encoder and modulator to increase the spectral efficiency. CM made it possible to associate several bits to a channel symbol. An example of CM systems is Trellis-coded modulation (TCM) that is a pair of a binary convolutional encoder and a memoryless modulator.
The main limitation of the CM schemes is that the channel encoder and modulator are designed jointly.[2] Instead, Bit-interleaved coded modulation (BICM) approach, added a bit interleaver to the chain of CM and placed it between the encoder and modulator. One of the best characteristics of BICM is that modulator and channel encoder can be selected independently, unlike the CM scheme. Due to this flexibility BICM is the most efficient and less constrained approach today.
Existence of the interleaver in BICM, helps increase the performance of the system, specially in the fading channels. This method first was shown in the paper by *Zehavi* [22]. In this paper, the proposed system tested over the fading channel (Rayleigh) and soft-decision is used at the Viterbi decoder. Later *E. Biglieri and G.Taricco* [5] provided the exact theory to evaluate the performance and design better systems. Currently, BICM is used in almost all modern communication systems like DVB-NGH, ATSC 3.0, 4G, and 5G in a combination of MIMO.
Today, the current studies are related to further optimize and improve this system. Thanks to BICM scheme and its flexibility to choose the modulator and channel encoder independently, this approach can be used to improve the spectral efficiency of the communication system by maximizing the capacity of the channel. Focusing on the modulator and the constellation used to map the information bits to the symbols, we don't even need to think about impacts of our work on the other blocks. So, we can assume that if we can achieve the highest possible capacity by moving the position of the constellation symbols, the resulting constellation is optimum one and must outperform the others.

1.2.2 Non-uniform constellations

Several attempts have been done by researchers to design optimized constellations for various systems. For example "Constellation design for memoryless phase noise channels" [11]. But the most recent one is a doctoral thesis by *M. Fuentes* [8] for ATSC 3.0. Great work has been done in BBC research and development center [19] in which the writer applied 1-dimensional optimization on the rectangular constellations and discussed many aspects of utilization of the resulting constellations like the possibility to use higher order constellations on the lower SNRs and their implications. Later, in addition to 1D, 2D optimization is done for both SISO and MIMO terrestrial broadcasting systems in [8]. In the same reference, complexity of demodulation is also has been discussed, and, appropriate and the most complete solution is provided.

1.2.3 Our approach

Our work is based on the references that are introduced in the previous section. In fact, we will try to cover the missing part of the previous works and accomplish them. For this reason, in this thesis, after design and implementation of the optimized non-uniform M-QAM (M stands for order) constellations, we will evaluate them in a real-world application. Also, the trade-offs of usage of these constellations will be discussed
For evaluation, first, we will set up the REDS chain simulator with proper modulator and demodulator functions applying the optimized constellations, then we will move towards Software-defined radio (SDR) implementation of the system, where the real hardware is attached to. At this point, we will perform tests and verify the results of the simulation. It must be mentioned that during the thesis, to save time we skipped the study of modulation under the order of 16 (16QAM) since they are near-optimal and there is not much space for optimization. We will discuss this later.

Chapter 2

Basics

2.1 System model

2.1.1 Transmission over channel

In digital transmission standards, the source must be converted to a bit-stream before being fed to the transmitter. According to the principle of the communications, if $s(t)$ is the continues-time signal sent by the transmitter over a channel, the received signal $y(t)$ is a combination of the channel response $h(t)$ and the additive white Gaussian noise $w(t)$:

$$y(t) = h(t) * s(t) + w(t) \tag{2.1}$$

Since nowadays almost all the communication systems are digital, it is needed to translate the above formula to the discrete-time form:

$$y[n] = h[n] * s[n] + w[n] \tag{2.2}$$

In this case, the information is transmitted every T seconds, so, the information rate R is $1/T$ (Hz), which corresponds to the signal bandwidth. Then, at the receiver side, the sampling rate should be set according to Nyquist criterion [15] to successfully extract the transmitted information from the received signal. Figure 2.1 shows a simple broadcast transmission model over a channel.

2.1.2 BICM blocks

As detailed in reference [5] and figure 2.2, the main blocks of a BICM system are Encoder, Interleaver, Mapper, Channel, Demapper, Deinterleaver, and Decoder. We will briefly describe relevant components in the next pages.

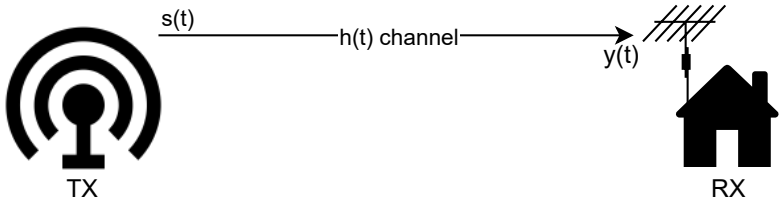

Figure 2.1: A simple terrestrial broadcasting system.

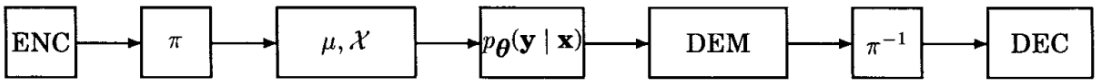

Figure 2.2: Block diagram of bit-interleaved coded modulation (BICM) scheme, π is bit-interleaver [5].

The transmission system blocks used in the REDS chain are the same as DVB–T, but with a different type of components. In the REDS chain, Reed-Solomon is cascaded by a Turbo coder which helps to remove the inner-interleaver comparing to traditional DVB–T to reduces the latency and increase the system performance.
Furthermore, they equipped the product with MIMO technology. The general block diagram of DVB–T transmitter is shown in the figure 2.3. One can easily distinguish the BICM part of this system. Here BICM components are Outer coder, Outer interleaver, Inner coder, Inner interleaver, and Mapper.

FEC and Interleaving

This component itself contains many other sub-components which cover most of the upper area in the block diagram 2.3.
The reference DVB–T system uses Forward Error Correction (FEC) to increase the error correction capability of the system. FEC block contains Reed-Solomon encoder with parameters (244, 188) as its outer encoder where the codeword length is 188 bits, and punctured convolutional encoder as its inner encoder.
The outer interleaving process is a convolutional byte-wise interleaving with depth $I = 12$. The Inner interleaving DVB–T uses a special block that is described in ETSI reference EN 300 744 v1.4.1 (2001-01).

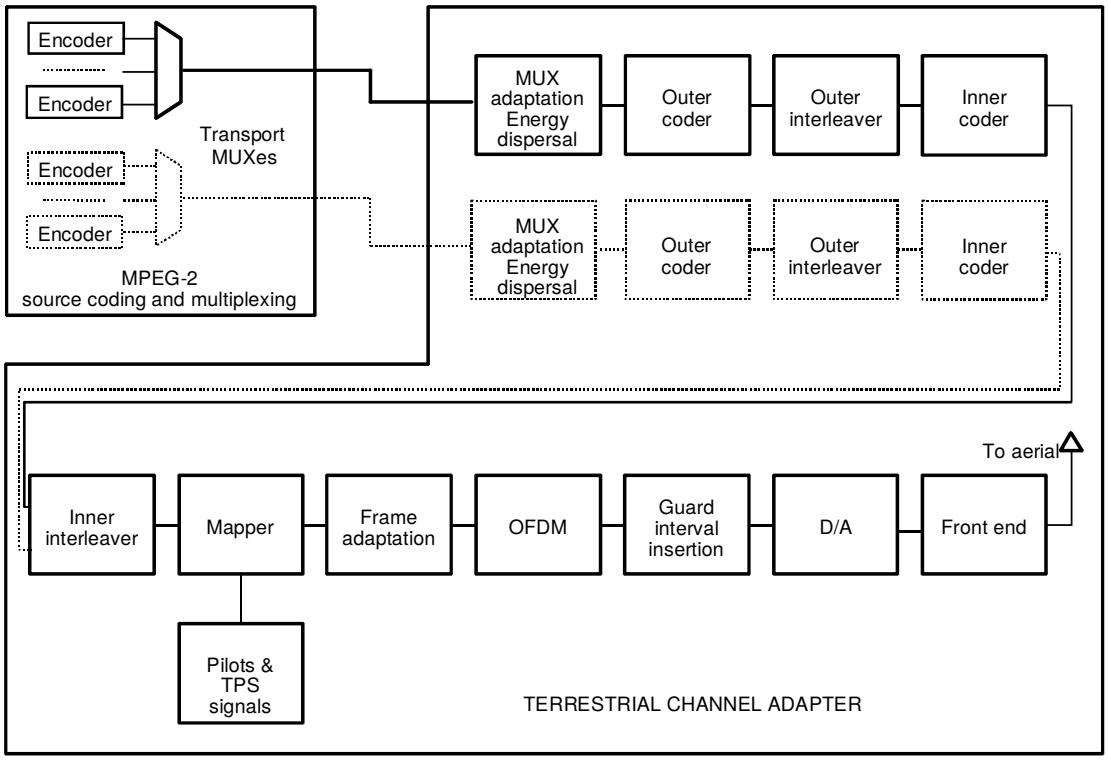

Figure 2.3: DVB–T block diagram of DVB–T [7].

Mapper

DVB–T is an old broadcasting standard that utilizes a Quadrature Amplitude Modulation (QAM) type of constellations in the modulator block, where the maximum order of constellation M is just 64. According to the standard, the possible Ms that can be used are 4, 16, and 64. The standard wants to normalize the power to the unit, so the "average power" normalization factor c is defined for each constellation order. The corresponding values for c equal to $1/\sqrt{2}$, $1/\sqrt{10}$, and $1/\sqrt{42}$, respectively.

OFDM Modulation

One of the most important and interesting elements in the DVB–T and REDS chain that recently is in use in any communication technology, is OFDM. With OFDM, the available spectrum is divided into several narrowband orthogonal subcarriers. OFDM brings many advantages to communication systems. Some of them are as follow:

1. As the frequency response of subcarriers (sub-channel) are overlapping, OFDM has higher spectral efficiency. But in the resulting spectrum, the maximum power on each subcarrier is located on nulls of other subcarriers (figure 2.4).

2. The subcarriers experience almost flat fading meaning that it mitigates multipath fading.

3. It eliminates the crosstalk, thus making it easier to design transmitter and receiver.

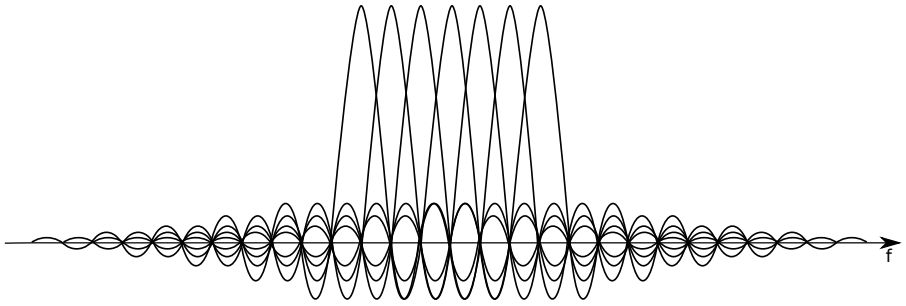

Figure 2.4: N OFDM subcarriers.

Figure 2.5 shows the discrete time model of OFDM as shown in [6]. According to the same reference, after several steps of calculations we have:

$$\begin{aligned} y_l &= DFT(IDFT(x_l) \circledast g_l + \tilde{n}_l) \\ &= DFT(IDFT(x_l) \circledast g_l) + n_l \end{aligned} \tag{2.3}$$

where $\circledast$ represents the circular convolution, y_l contains N received data point, x_l is the N transmitted constellation points and g_l the channel impulse

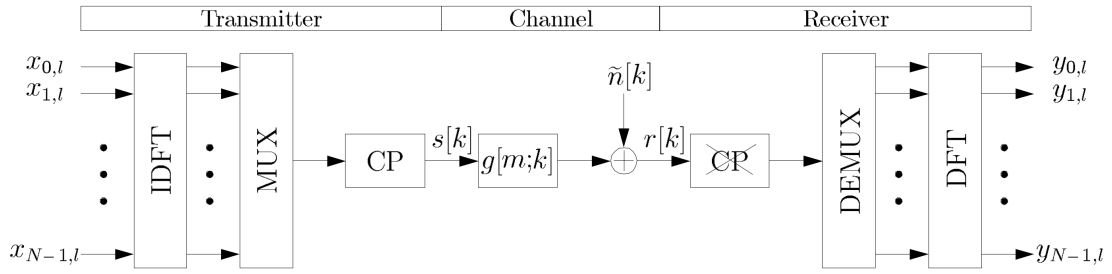

Figure 2.5: OFDM system used in digital communication systems. Note that CP stands for Cyclic Prefix.

response. Assuming the channel noise $\tilde{n}_l$ is white and Gaussian, n_l is the uncorrelated Gaussian response. Considering that DFT of two cyclically convolved signals is the product of their individual DFTs, we can rewrite the above equation as below. Note that DFT(g_l) is the frequency response of the channel.

$$y_l = x_l.DFT(g_l) + n_l \tag{2.4}$$

which means using the fast Fourier transform (FFT), DFT and IDFT can be done at a high speed in transmitter and receiver.

2.1.3 Reception

AT the receiver after time and frequency synchronization, all the blocks in the transmitters diagram must be reversed in order to get the original bits. To increase the performance, instead of Hard decoding the demapper uses the Approximate Log-Likelihood Ratio algorithm with Viterbi decoder to demodulate the received data. Soft Viterbi decoder is used to decode the coded data by the convolutional encoder.

2.2 Capacity of a communication channel

2.2.1 Shannon theorem

In the equation 2.2 if the only disturbance in the channel is AWGN noise, the $h[n]$ can be assumed to be 1. So the equation can be simplified to:

$$y[n] = s[n] + w[n] \tag{2.5}$$

where $w[n]$ is white additive Gaussian noise with zero mean and variance (noise power) of σ^2. According to the Shannon theorem the Capacity C of this channel can be expressed as the below equation, where P is the average power of the signal and W is the channel bandwidth.

$$C(bit/s) = W \log_2 \frac{P + \sigma^2}{\sigma^2} \tag{2.6}$$

One can simplify this equation to have Signal to Noise Ratio SNR in it; where $SNR = P/\sigma^2$.

$$C(bit/s/Hz) = \log_2 (1 + SNR) \tag{2.7}$$

which results the figure 2.6. Basically, Shannon capacity is the upper bound for transmission rate at a certain SNR.

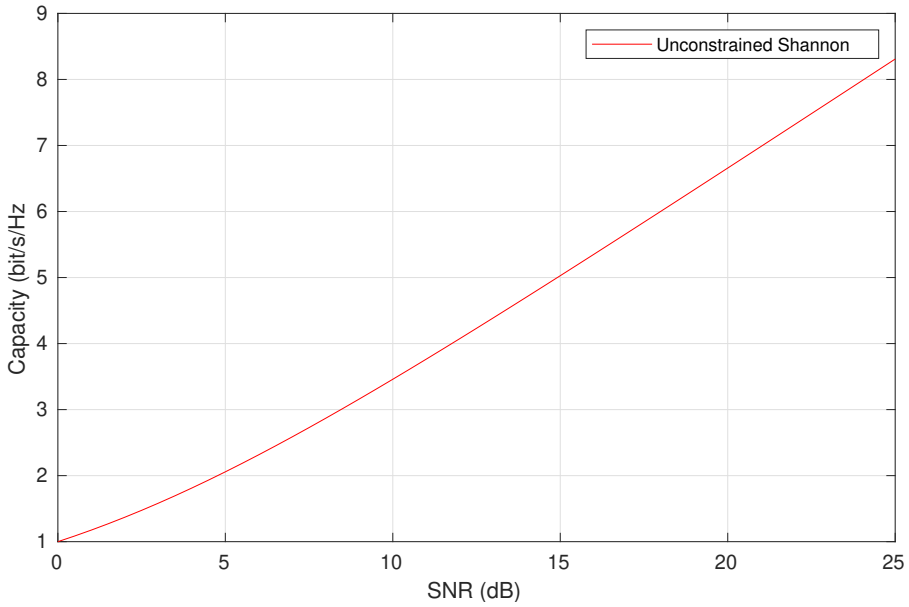

Figure 2.6: Shannon capacity limit AWGN channel.

2.2.2 CM and BICM Capacity

As described in section 1.2.1, CM and BICM systems are very useful to obtain overall higher system performance. Since in communication systems the channel is not ideal ($h[n] \neq 1$), a powerful channel coding is needed in addition to Interleaving, which are used to minimize the error bursts so that the erased bits can be recovered at the receiving end [22].
From reference [5], when the receiver signal is $y = hx$, then the BICM system can be modeled as a m parallel binary input channels (figure 2.7). the CM and BICM capacities can be calculated as follows:

$$C_{CM} = I(x; y|h) = m - \mathbb{E}_{x,y,h}\left[\log_2 \frac{\sum\limits_{x' \in \chi} p(y|x', h)}{p(y|x, h)}\right] \tag{2.8}$$

where $E_{x,y,h}$ denotes the expectation with respect to s, y and h; χ is the set of constellation symbols; $m = log_2(M)$ is the number of bits per constellation symbol. Remember that also m is the number of the parallel channels in the equivalent model and each m corresponds to a position in the label of the

constellation χ.

$$C_{BICM} = I(c_l; y|h) = m - \sum_{l=1}^{m} \mathbb{E}_{x,y,h} \left[\log_2 \frac{\sum\limits_{x' \in \chi} p(y|x', h)}{\sum\limits_{x' \in \chi_l^b} p(y|x', h)} \right] \tag{2.9}$$

In this equation, the term χ_l^b denotes the set of symbols in a constellation χ that the coded bit c_l is equal to $b \in \{0,1\}$. Also, $p(y|x,h)$ is the conditional probability density function (pdf). This expression holds in general for all kinds of channels, AWGN, Rayleigh, or Rician. Also $C_{CM} \geq C_{BICM}$. But it must be noted that despite the performance loss in BICM, iterative decoding shows significant improvements.

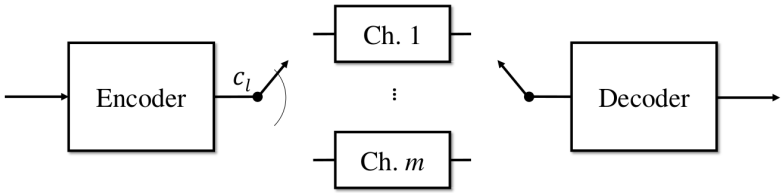

Figure 2.7: Equivalent BICM system model [8].

2.3 Improvements in REDS transmitter

[] In the REDS transmission chain, two methods were adapted comparing to the original DVB–T to increase the data rate: The most noticeable and important changes are: using higher QAM constellations in the Modulator, and transforming the existing SISO to MIMO technology.

Technically, the QAM constellation order M increased from 64 to 256. This is a very reasonable method to increases the data rate of the system, but the downside of this is degradation in the Bit Error Rate (BER) performance of the system.

To avoid the BER degradation, one can think of increasing the transmission power or using the powerful channel encoding. According to the application and requirements of the project, increasing the transmission power is not a valid solution. So, the remaining option is that the convolutional encoder and Viterbi decoder must be replaced by a Duo-Binary encoder and decoder. Since the duo-binary turbo encoder includes an interleaver block, the coexistence of this interleaver with the inner interleaver in the transmission chain will increase the system latency. According to the documentation of the

project [1], the performed simulations showed that eliminating the inner interleaver does not impact the system's overall performance at the end. Thus removing it can decrease the latency.
Figure 2.8 shows a simplified block diagram of the REDS transmission chain used for both simulation and evaluation.

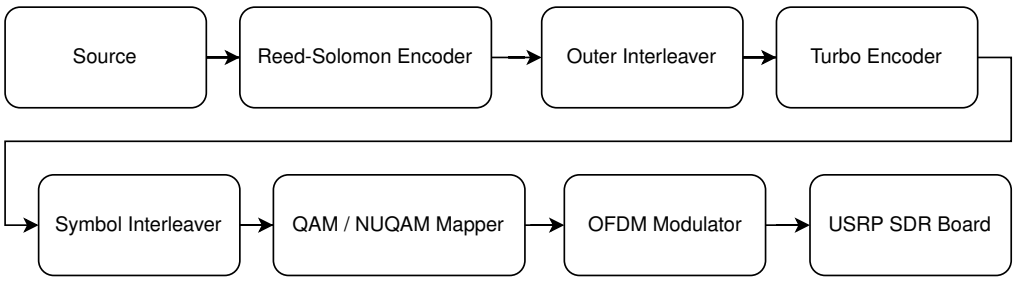

Figure 2.8: Simplified REDS transmission chain.

2.3.1 Further improvements

So far all the preliminaries for starting to discuss the optimization are explained. For most of the optimization, the BICM capacity function is used to achieve the optimal positions of the constellation symbols in the considered M–QAM constellations. As mentioned before, M is introduced by the requirements of the project and is equal to 4, 16, 64, and 256 values.

Here, the question may arise: Why the BICM capacity equation is used for optimization? The answer is that because it is a valid description for the channel capacity in the system under study. Moreover, by using this equation, one can avoid the many associated parameters required for calculations to get the BER values.
This way is indeed much faster than the association of all blocks and their parameters in the chain for doing the calculations. We know that maximizing the BICM capacity function translates to have a small number of errors (in terms of BER) at the receiver side. As a result, this leads to less power consumption for achieving a certain BER. Because the Quasi Error Free (QEF) value can be reached in the lower received SNR. It must be mentioned that for the DVB–T standard $QEF = 2 \times 10^{-4}$, after the Viterbi decoder.

Part II

Optimization and Result

Chapter 3

Optimization

3.1 Comparison of PSK, APSK and QAM

Before continuing, it is worth mentioning a fact about choosing between [A]PSK and QAM.
In PSK the transmitter can operate at the maximum power, but in QAM it is not possible to use the maximum power to send the symbols that their amplitude are less than the maximum power. Also one can think of using APSK, in this case, given a modulation order, APSK could have less amplitude levels that leads to a lower peak-to-average power ratio (PAPR).

But in terms of spectral efficiency, QAM wins as in our case the distance between transmitter and receiver in the system under study is not as long as distance in satellite communications.

3.2 BICM capacity maximization

According to the reference [5], BICM capacity can not be calculated in closed form, so the method described in reference [16] is used for numerical computation. For a modulation encoding m bits per second, the BICM capacity for an SNR value γ can be calculated as:

$$C_{BICM} = I_m(\gamma) = m - \mathbb{E}\left[\frac{1}{m}\sum_{i=1}^{m}\sum_{b=0}^{1}\sum_{z\in\chi_b^i}\log_2\frac{\sum_{x\in\chi}\exp\left(-|Y-\sqrt{\gamma}(x-z)|^2\right)}{\sum_{x'\in\chi_b^i}\exp\left(-|Y-\sqrt{\gamma}(x'-z)|^2\right)}\right] \tag{3.1}$$

where χ is the set of 2^m constellation symbols, χ_b^i denotes the set of the symbols for which bit i equals to b, and Y is a complex normal random

variable with zero mean and unit variance. Using enough N realizations of Y, one can produce smooth curves and reliable results.

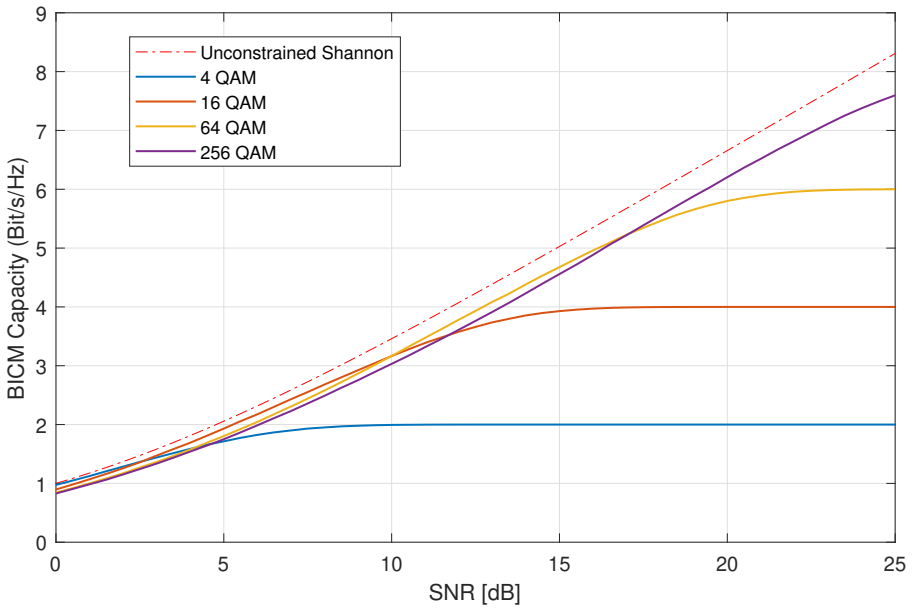

Figure 3.1: BICM capacity for 4, 16, 64 and 256 QAM (AWGN channel).

Figure 3.1 indicates the Shannon capacity limit (equation 2.7) and BICM capacity (equation 3.1) of uniform 4, 16, 64 and 256 QAM constellations. When using uniform QAM, according to this figure, there is a best performing uniform QAM constellation in a certain range of SNR. For example in a SNR range of [3,10], it is better to use 64QAM since its gap to the Shannon limit is less than the others in that range.
Another result of figure 3.1 which is important for this thesis is observing the gap and available optimization space for each constellation at each SNR value. According to figure 3.2 which shows the shortfall from Shannon capacity for the different order of uniform QAM constellations, the gap from the Shannon capacity increases with SNR and constellation order M.
Based on these findings and the requirements of the system under study, this thesis at the first stage focuses on doing optimization, e.g. maximizing the BICM capacity in certain SNR ranges where DVB–T QEF condition can be reached by the system. This way, the dependency on many parameters of the system will be eliminated to achieve reliable results. As mentioned in previous sections, maximization of BICM capacity is equal to error reduction and hence better BER performance. Therefore it is reasonable to consider only certain constellation orders. Note that QEF value for DVB–T

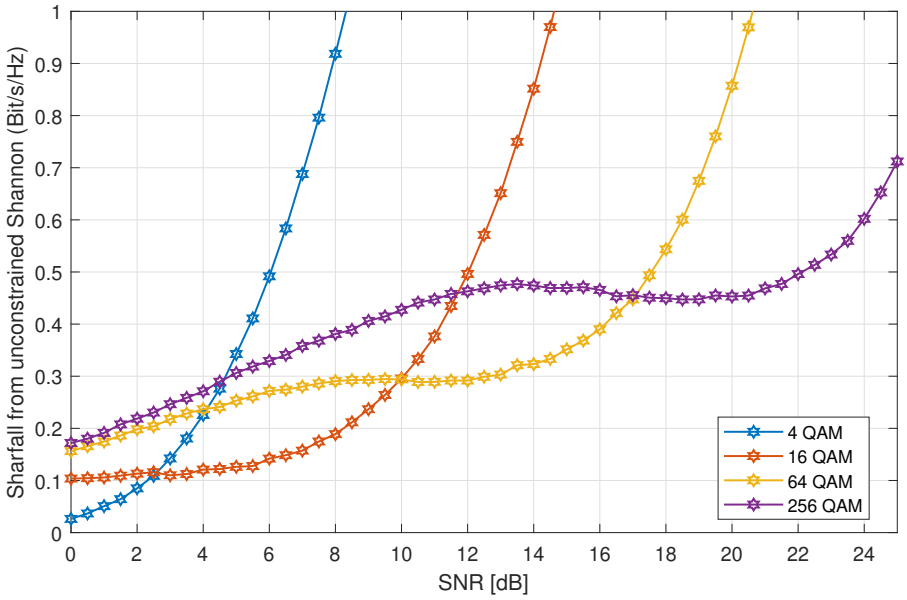

Figure 3.2: BICM capacity shortfall from Shannon capacity for M = 2, 4 ,6, 8 (AWGN channel).

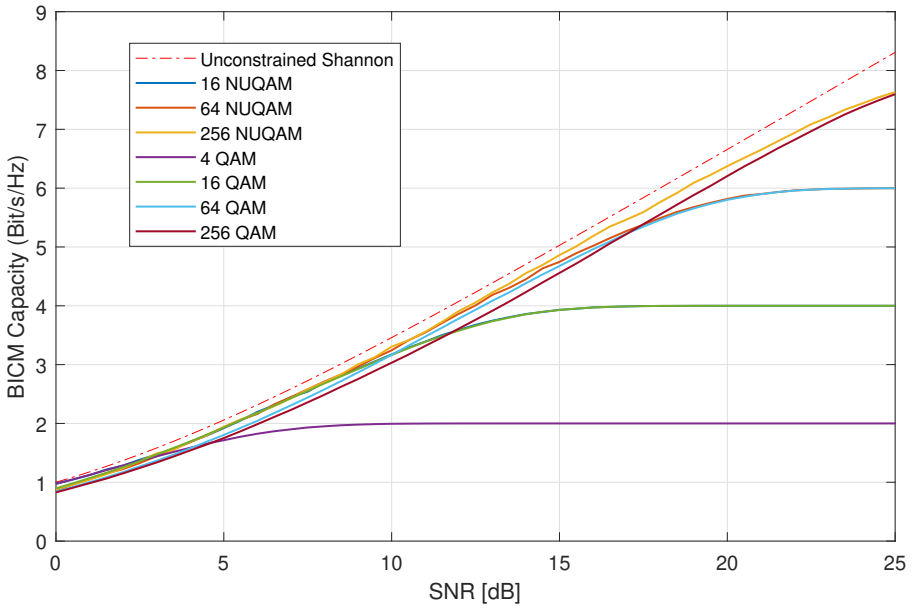

Figure 3.3: BICM capacity for 4, 16, 64 and 256 QAM and NU–QAM constellations (AWGN channel).

equals 2×10^{-4} at the output of the inner decoder which is Turbo in the REDS transmission chain. This value means less than 1 uncorrected error

per hour.

In figure 3.3, BICM capacity is calculated for original QAM and 1D–NUQAM constellations using equation 3.1 in a range of SNRs. In this figure the optimal positions are extracted from reference [19]. This is showing clearly the superior behaviour of 1D–NUQAM constellations comparing to uniform one.

3.3 Optimization process and algorithm

For maximization of the BICM capacity described in the section 3.2, a non-linear numerical optimization method must be employed since all the calculations are numerical. Based on the trials, the best performing optimization algorithm for our goal was Nelder–Mead optimization method (NM) that is described and discussed completely in [12].

In our case, the generic form of the optimization formula is as equation 3.2. NM inputs POS_{Init}, a set of initial M–ary constellation symbol positions as starting parameter values in addition to $NM_{Options}$, a set of options like power level in which the optimization must be done. The output POS_{Out} is a set of optimal positions in the I–Q plane, where the BICM capacity function is maximized. Of course, the NM is for finding the minimum of a function; therefore to get the maximum we need to invert the BICM capacity function.:

$$POS_{Out} = NM(-1 \times C_{BICM}, POS_{Init}, NM_{Options}) \tag{3.2}$$

A pseudo-code to demonstrate the NM algorithm is shown in Algorithm 1. In figure 3.4 a graphical representation of the algorithm 1 is provided. In addition an example of applying NM on a nonlinear function to find its minimum is depicted in figure 3.5.

3.4 Demapper

The Maximum-Likelihood (ML) demapper is used to minimize the errors. For ML, for each received bit the Log Likelihood Ratio (LLR) [20] can be computed as:

$$L(b) = log\left(\frac{Pr(b=0)|r=(x,y)}{Pr(b=1)|r=(x,y)}\right) \tag{3.3}$$

Algorithm 1: Nelder–Mead optimization method (NM) Algorithm

input : A function f, a vector x and termination conditions (σ_1, σ_2)
output: Optimal parameters values minimizing function f

Create a simplex of $n+1$ points for n–dimensional vectors x;
while $x_{n+1}^{current} - x_{n+1}^{previous} < \sigma_1 and\ f(x_{n+1}^{current}) - f(x_{n+1}^{previous}) < \sigma_2$ **do**
  Order: $x_1 < ... < x_{n+1}$ such that $f(x_1) < ... < f(x_{n+1)}$;
  Reflect: $x_r = 2m - x_{n+1}$, $m = \Sigma x_i/n, i = 1...n$;
  if $f(x_1) \leq f(x_r) < f(x_n)$ **then**
    $x_{n+1} = x_r$; Goto next iteration;
  end
  if $f(x_r) < f(x_1)$ **then**
    Expansion: $x_s = m + 2(m - x_{n+1})$;
    if $f(x_s) < f(x_r)$ **then**
      $x_{n+1} = x_s$; Goto next iteration;
    else
      $x_{n+1} = x_r$; Goto next iteration;
    end
  end
  if $f(x_r) \geq f(x_n)$ **then**
    Contract:;
    if $f(x_r) < f(x_{n+1})$ **then**
      Contract outside: $x_c = m + (x_r - m)/2$;
      if $f(x_c) < f(x_r)$ **then**
        $x_{n+1} = x_c$; Goto next iteration;
      else
        Goto Shrink;
      end
    else
      Contract inside: $x_c c = m + (x_{n+1}) - m)/2$;
      if $f(x_c) < f(x_r)$ **then**
        $x_{n+1} = x_{cc}$; Goto next iteration;
      else
        Goto Shrink;
      end
    end
    Shrink: $v_i = x_1 + (x_i - x_1)/2$, $f(v_i), i = 2...n+1$;
  end
end

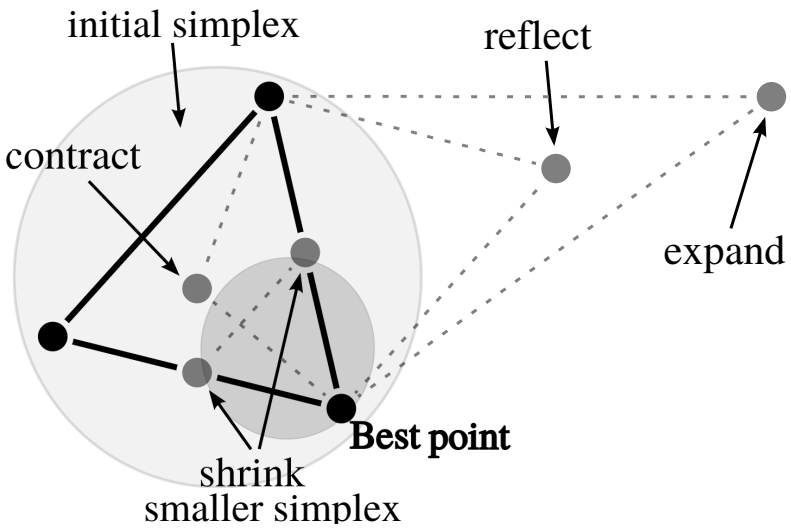

Figure 3.4: Evolution of the initial simplex in NM algorithm.

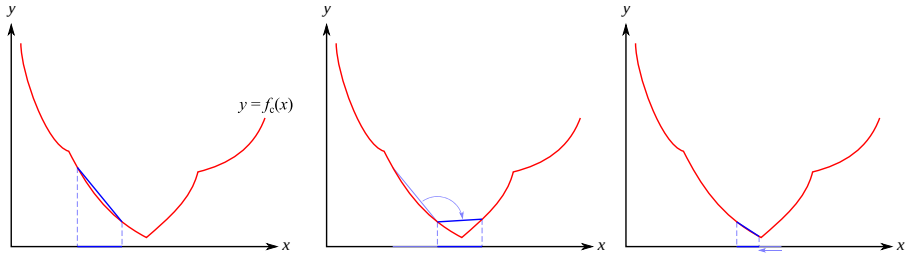

Figure 3.5: Nelder-Mead optimisation method in a one-dimensional space. Initial situation (left), reflection of the simplex (middle) and contraction of the simplex (right) [21].

assuming that the transmitted symbols are equally probable and that the noise follows a Gauss distribution:

$$L(b) = log\left(\frac{\sum_{s\in S_0} e^{-\frac{1}{\sigma^2}\left((x-s_x)^2+(y-s_y)^2\right)}}{\sum_{s\in S_1} e^{-\frac{1}{\sigma^2}((x-s_x)^2+(y-s_y)^2)}}\right) \tag{3.4}$$

In this equation, x and y are the coordination of received constellation symbol, and s_x and s_y are the reference coordination. Also, s_0 and s_1 are the ideal symbols or constellation points with bit 0 and 1 at the given bit position, respectively [10].
Approximate LLR is computed by taking into consideration only the nearest constellation points to the received signal, rather than all the constellation

points (as done in exact LLR); We have as in reference [10]:

$$L(b) = -\frac{1}{\sigma^2}\left[\min_{s\in s_0}[(x-s_x)^2+(y-s_y)^2] - \min_{s\in s_1}[(x-s_x)^2+(y-s_y)^2]\right] \quad (3.5)$$

When it comes to the complexity of demapping, it is known that the complexity degree for 1D–NUQAM is the same as uniform QAM. But, as described in DVB–T2 standard, for more efficiency, QAM constellations can be used with rotation and cyclic Q-delay. Then, one can think about using 2D–NUQAM together with rotation. Because using cyclic Q-delay requires the demapper to consider the 2 axes in the plane and this means that the complexity is already increased. By implementing such a demapper to benefit from Q-delay, it must already have enough capability to be used with 2D–NUQAM. We will discuss this more later.

Chapter 4

Non–uniform QAM

4.1 1D Optimization

For a M–ary QAM constellation with order M, the position of constellation symbols can be represented as a set of $[x, y]$ on the I-Q plane and be produced by the all 2-by-2 combination of coordination set D that is:

$$D = \{-a_n, -a_{n-1}, ..., -a_1, -1, +1, a_1, ..., a_{n-1}, a_n\} \tag{4.1}$$

where n is equal to $\frac{\sqrt{M}}{2} - 1$, and is called the number of parameters which must be optimized: Degree of freedom (DOF). Note that because the power normalization ± 1 is a fixed position, so we would associate it as a parameter for optimization.
Now, the optimization process is to find all the x and y pairs belonging to all symbol positions of a constellation with certain M, that maximizes the corresponding BICM capacity or equivalently Mutual Information I for a given received signal to noise power ratio. In fact, The optimization tries to find a specific constellation for each SNR in which BICM capacity reaches its global maximum.
To minimize bit errors between adjacent symbols, Gray coding is applied in the design of constellation symbols. Because by Gray labeling each symbol has just one nearest neighbor.
In figure 4.1 the evolution and movements of the constellation points are shown for the two M values of 64 and 256 at SNR of 9 [dB] when the channel is AWGN.

In the next sections, the discussion of the optimization process is followed by a MATLAB simulation of the resulting constellation using the REDS transmission chain, and the corresponding BER curves are depicted.

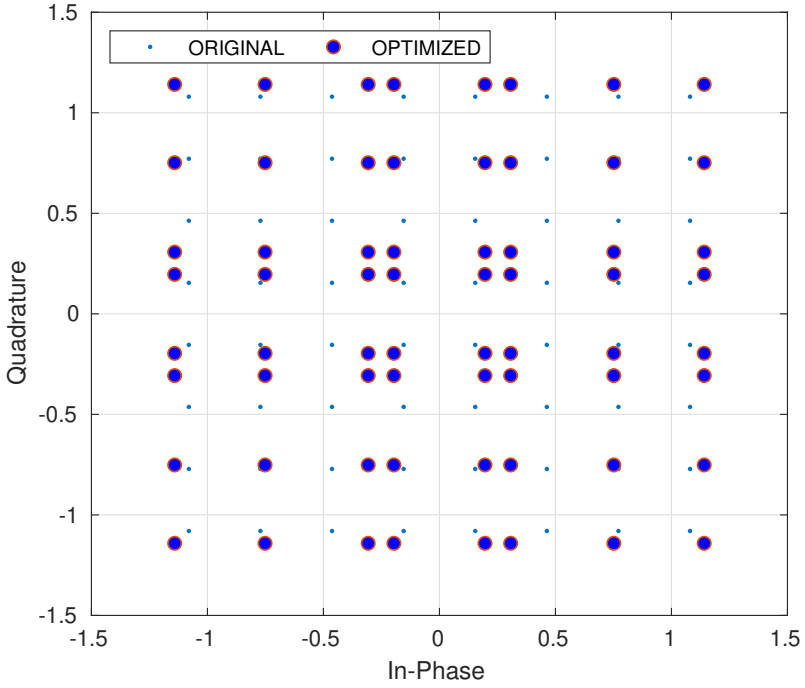

Figure 4.1: a: QAM and optimized Non-Uniform constellations for SNR=9 and $M = 64$. b: Optimized Non-Uniform constellations for SNR=12 and $M = 256$.

4.1.1 64 1D-NUQAM

For $M = 64$, different optimization settings are available that will be discussed and compared later.
For the first attempt, using the basics explained in section (4.1) we have DOF $= 3$ which means that the parameters to be optimized are a_3, a_2 and a_1 corresponding to $\pm 7, \pm 5, \pm 3$ both in I and Q plane. This will keep the rectangular shape of the constellation.

First, the optimization algorithm must be initialized. To do this, instead of letting the optimizer choose random positions, the best idea is to enter values for parameters close to the uniform 64QAM.
By starting the process, based on the speed of the computer processor, after many iterations, the function reaches a global maximum. The evolution of these parameters with respect to SNR values is depicted in figure 4.2. It is noticeable that the inner symbol positions do not change after arriving at SNR $= 14$, while the outermost ones are experiencing the most of the

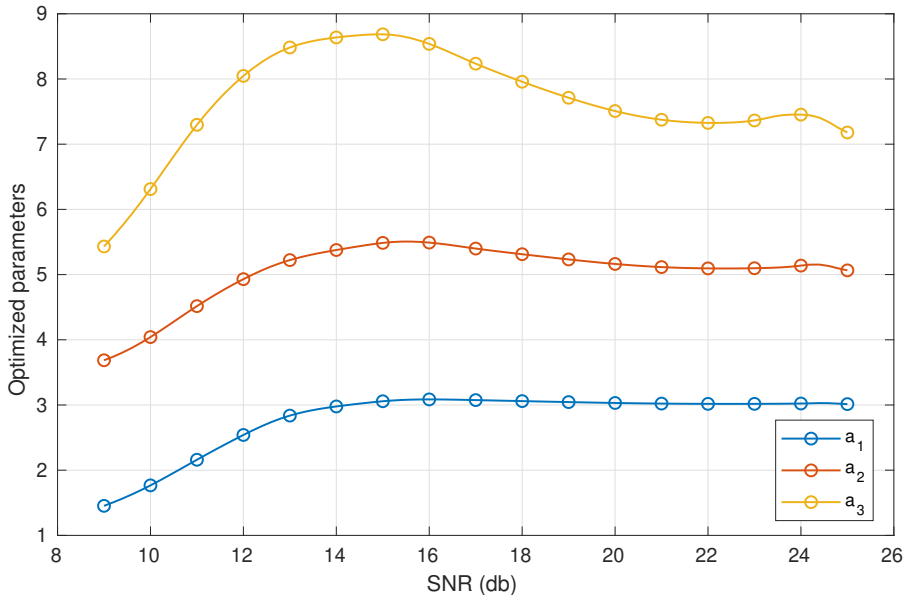

Figure 4.2: The evolution of values of 64 1D-NUQAM parameters.

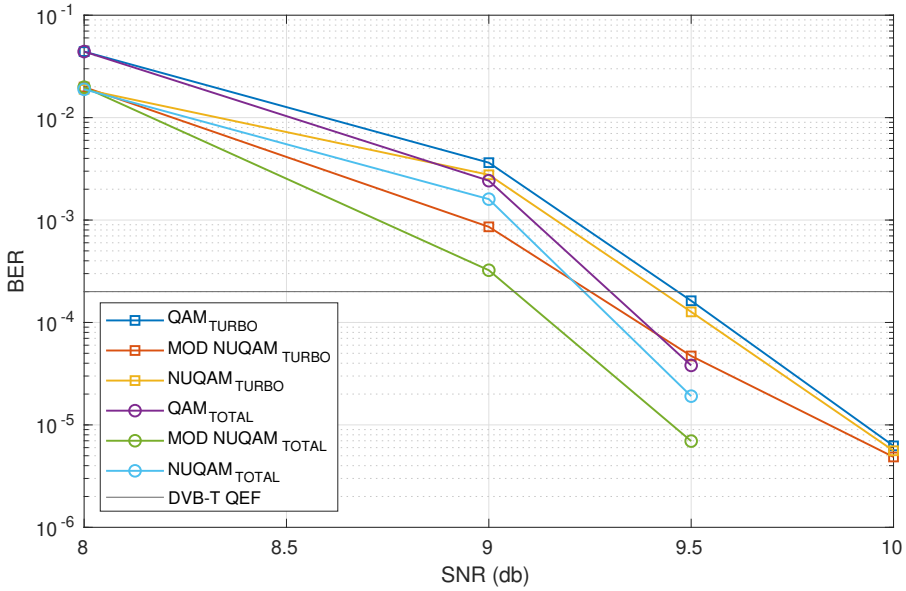

Figure 4.3: BER of original and optimized 64QAM for SNR = 8, 9, 9.5 and 10.

variations.

Figure 4.3 shows the simulation results using the model in figure 2.8 in terms of BER curves for SNR 8,9, 9.5 and 10 where QEF happens somewhere between these SNRs when Code Rate (CR) is 1/3. In this figure, the first 3

curves show BER at the output of Turbo decoder, and the latter 3 curves are for the output of the Reed-Solomon, which can be called the total BER of the system; as Reed-Solomon is the last block in the receiver before retrieving the data. Here, the curves are drawn for $M = 64$ QAM and 1D–NUQAM constellations. The gray horizontal line is related to DVB–T QEF.
Note that there are two sorts of BER curves in this figure; some correspond to the resulting constellation by the optimizer and the others are labeled as "MOD NUQAM". Looking at this figure, one can see a small improvement using "MOD NUQAM".
MOD NUQAM curves are obtained by manually manipulating (increasing) the third optimized parameter value. Although it has slightly better BER performance, the consequence is a reduction of the capacity. Actually, these are non–optimized constellation whenever both of the BER and capacity factors are considered jointly. So making one better, worsens the other. But, the important point is that by this manipulation, still both of the capacity and BER are reaching a better value than the uniform QAM. For example, assuming SNR = 9 [dB], CR = 1/3 in *Rayleigh condition* we have table 4.1. In the last row (MOD 64 1D-NUQAM) it can be seen that the BER is better than the second row, but with the cost of losing 0.03 units of capacity. As mentioned before, it has still a better BER performance and Capacity in comparison to uniform QAM.

Constellation	**1, a_1, a_2, a_3**	**Capacity**	**BER**
Uniform 64 QAM	1, 3, 5, 7	2.86	3.633757e-03
64 1D-NUQAM	1,1.45, 3.69, 5.42	2.96	2.267724e-03
MOD 64 1D-NUQAM	1, 1.45, 3.69, 7	2.93	1.753132e-04

Table 4.1: Capacity (Bits/Hz/s) and BER at the output of the Turbo decoder.

4.1.2 256 1D-NUQAM

For $M = 256$ the number of parameters DOF is 7. This will impact the optimization time, making it longer. Here, an applied trick to the initialization part in order to minimize the optimization process time is using the optimized value for the current SNR as initial values for the next SNR, given that the distance between the two consecutive SNR values is small. Otherwise, it won't be effective.

Like the previous case, we need to define the input parameters a_n: ±15, ±13, ±11, ±9, ±7, ±5, ±3. Figure 4.5 shows the position of the symbols in 256 1D–NUQAM; We can see that if SNR increases, the shape of the constellation tends to be a uniform QAM, e.g. $SNR > 24$.
Another figure 4.4 shows the BER curves resulted from the simulation of REDS transmission system in MATLAB at Rayleigh condition and code rate of 1/3 with 256 1D–NUQAM and 256 QAM. In this case, QEF can be reached in higher SNR, and therefore there is more gap to the Shannon limit. Comparing the two curves QAM_{TURBO} and $NUQAM_{TURBO}$ where they cross the QEF (horizontal line), a 0.8 [dB] gain can be seen. This is also true for the total BER of the system. This means that we are able to close the gap between the QAM constellation and Shannon limit using optimal constellations.

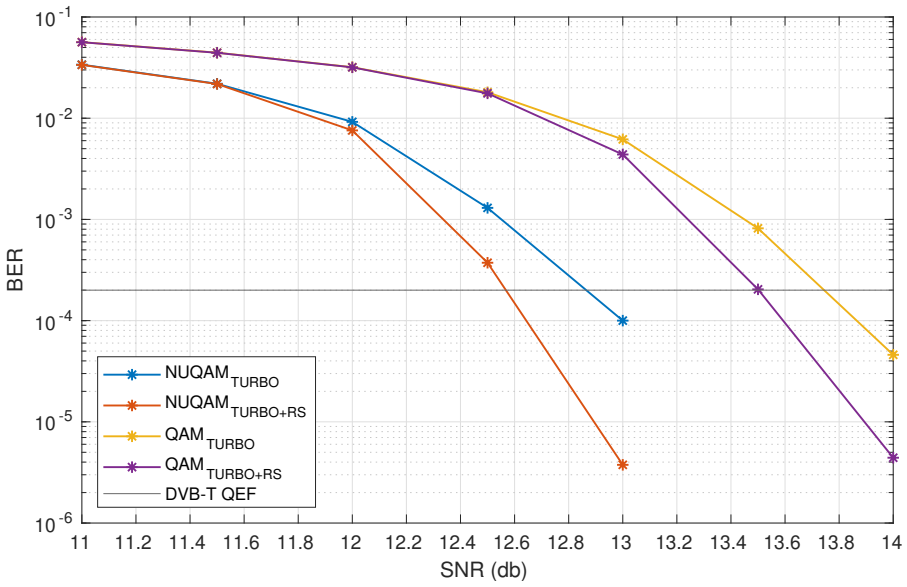

Figure 4.4: BER of original and optimized 256QAM for SNR range of 11 – 14.

4.2 2D Optimization

A further step after 1D optimization is performing the optimization in 2 dimensions. Obviously, we should expect overall better performance for our transmission system and more power gain. Because in this case, all the constellation symbol positions are free to move in both x and y direction, which

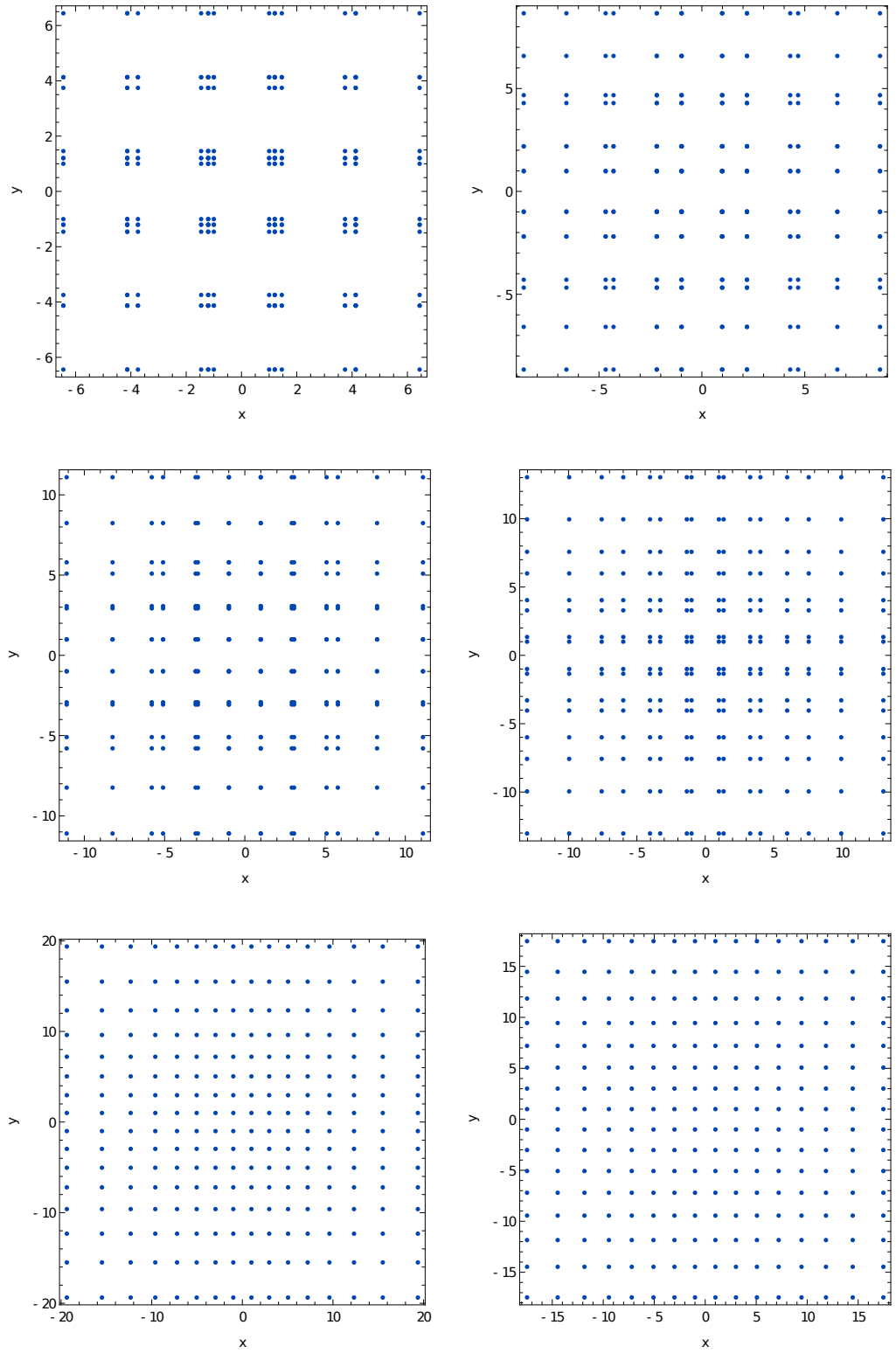

Figure 4.5: 1D–256NUQAM in different SNRs: from top left to right SNR = 9, 12, 15, 18, 21 and 24 respectively [19].

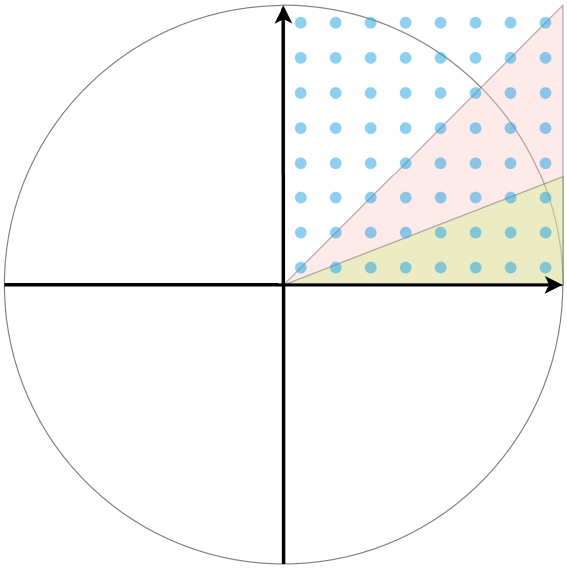

Figure 4.6: Example of using symmetry for 256 2D–NUQAM: blue points show 1/4, the red section is 1/8, and green is 1/16 of the whole I/Q plane.

means that the resulting constellations are not obliged to keep the initial rectangular shape. During the optimization procedure, the optimizer will force them to move to the coordination in which the given BICM capacity is maximum.
Having more freedom of movement leads the optimizer to have many parameters. Therefore the DOF will be increased massively. Now each constellation symbol has 2 parameters to be optimized.

One of the methods to simplify the model and speeding up the optimization procedure and saving time is to use the symmetric feature of the QAM constellations. Indeed we are going to consider only those symbols which are located in one quadrature. We can even divide one quadrature again and use 1/8 of the I/Q plane and so on so forth. Therefore, we can generate the rest of the points by remapping the optimized positions to the rest of the I/Q plane. Figure 4.6 represents this concept.
Besides the mentioned simplification method, we applied the same technique used for the 1D case for further time saving: once the optimal points are obtained for the current SNR value, they can be used as initialization location for the next close SNR.

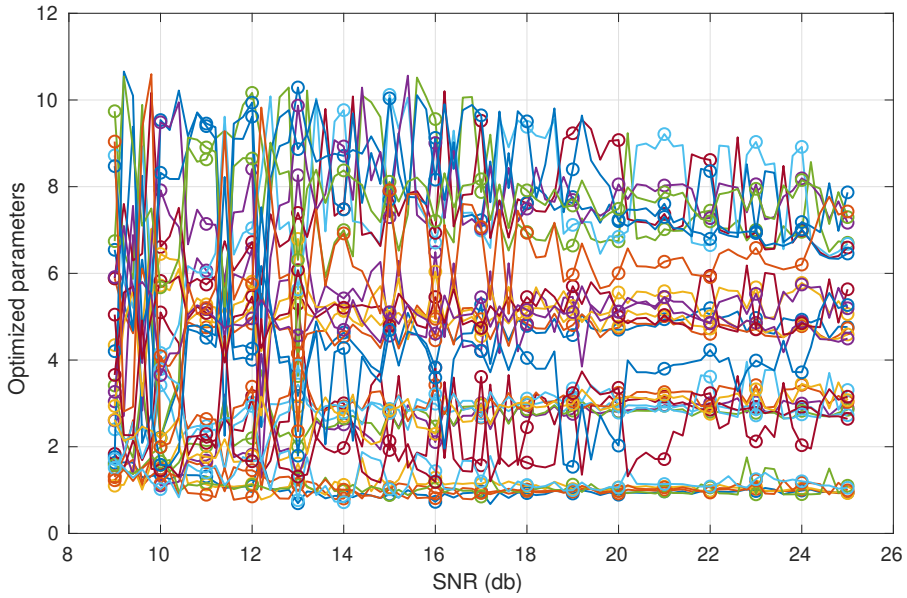

Figure 4.7: Illustration of the evolution of values of 64 2D-NUQAM parameters.

4.2.1 64 2D-NUQAM

Assuming the use of 1/4 of the I/Q plane, the DOF for 2D optimization is equal to $\frac{M}{2} - 1$. If $M = 16$, the number of parameters to be optimized is 30, fixing the position [1,1].

Figure 4.7 is just for illustration of a very complicated evolution behavior of the middle and outer points in 64 2D–NUQAM within the SNR range of 9 to 25 dB, while the inner points are almost merged.

The resulting constellations are depicted in figure 4.8, for SNR values of 8 to 24 with step size = 2. In lower SNRs like 8 [dB] some symbols and especially inner ones remind the "Condensed" concept discussed in section 4.2.4. Instead as SNR increases, the symbols start to split.

Simulation results in MATLAB show superior BER performance of the 64 2D-NUQAM over uniform 64QAM in Rayleigh condition and CR of 1/3 (figure 4.9). Comparing these BER curves with the ones at figure 4.3 where they cross QEF criterion, we can see about 0.5 [dB] more gain for 2D optimization than 1D optimization. Also, we have about 0.6 [dB] gain comparing to uniform 64QAM.

In the next figure 4.10, CR is changed to 3/4, and still, the previously mentioned performance result holds, but this time the difference between 1D and 2D optimized constellation is negligible.

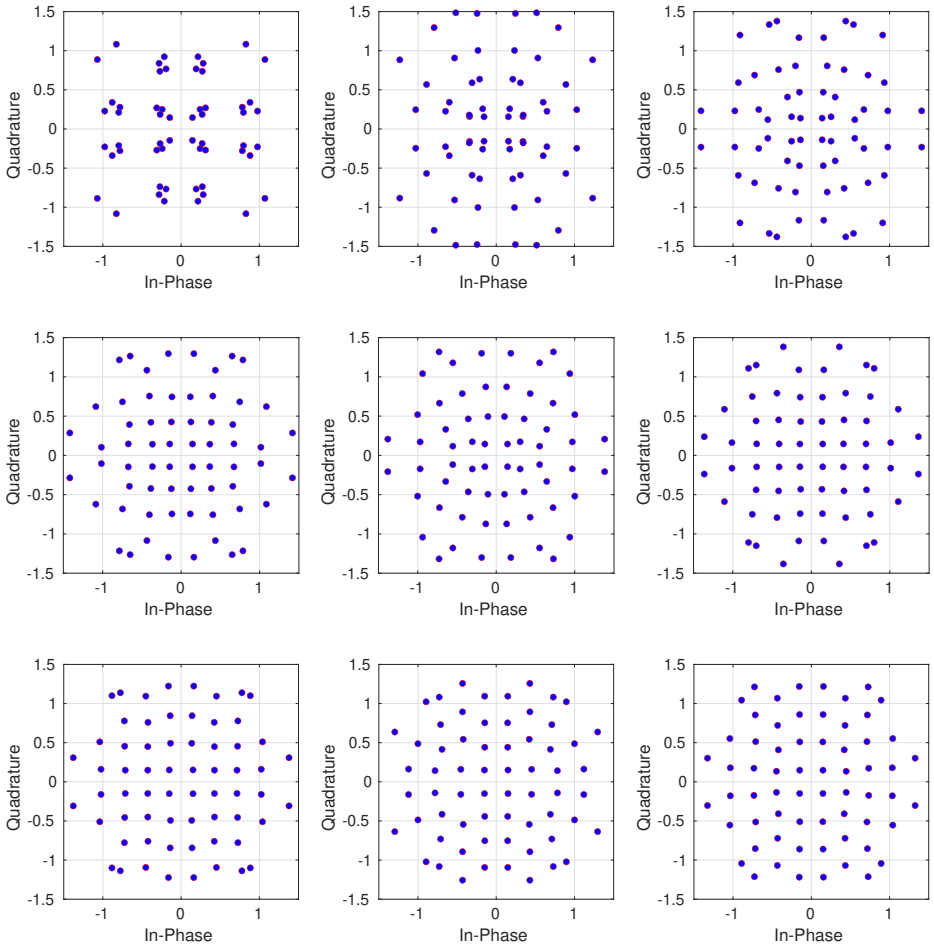

Figure 4.8: Optimized 64 2D–NUQAM for SNR values of 8, 10, 12, ..., 24 from top left to right.

4.2.2 256 2D-NUQAM

The 2D optimization process for M = 256 must be modified to decrease the huge number of parameters to speed up and simplify the process, otherwise, it would be very cumbersome. Having many parameters, it is highly probable that the optimizer will fall into local minima. To avoid this problems, if we follow the same process used in 64 2D–NUQAM (considering only one quadrant), we get DOF = 128. Using MATLAB, this will take about 4 days with a middle range desktop CPU to obtain the result, which is not feasible.

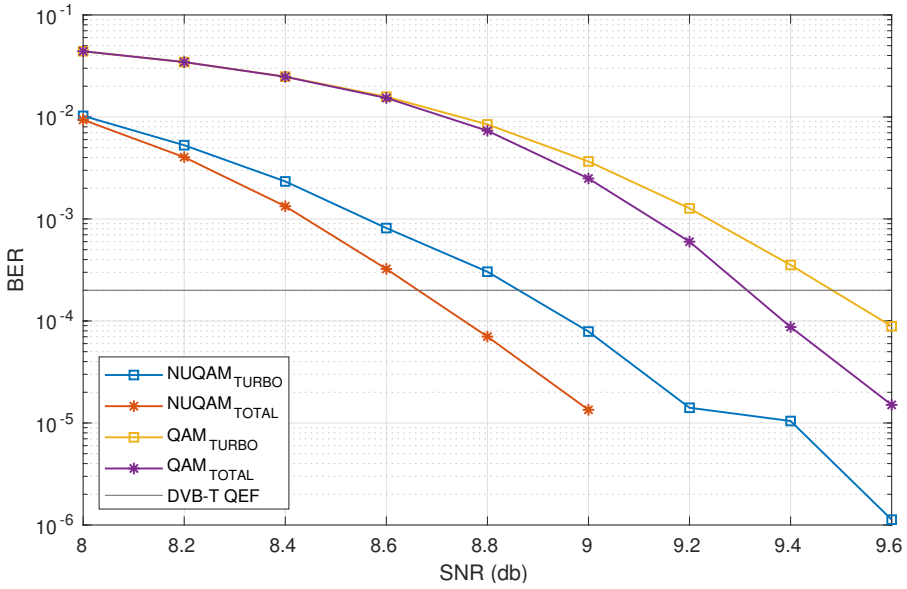

Figure 4.9: Performance of 64 2D–NUQAM in Rayleigh channel and CR of 1/3.

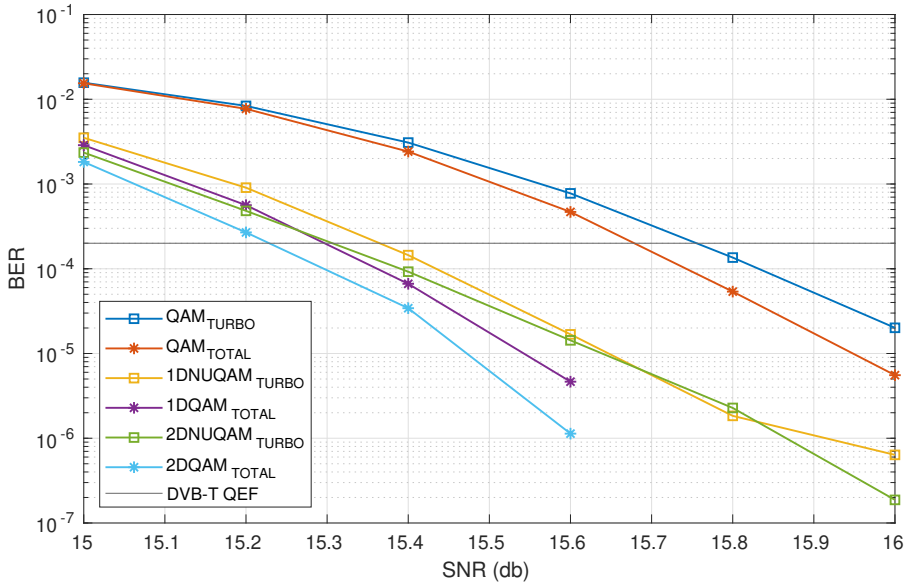

Figure 4.10: Performance of 64 2D–NUQAM in Rayleigh channel and code rate 3/4.

So, considering another level of symmetry, which is 1/8 of the constellation symbols in the I/Q plane, allows us to do optimization and later we map the resulting symbol positions to other sections to get a full constellation.

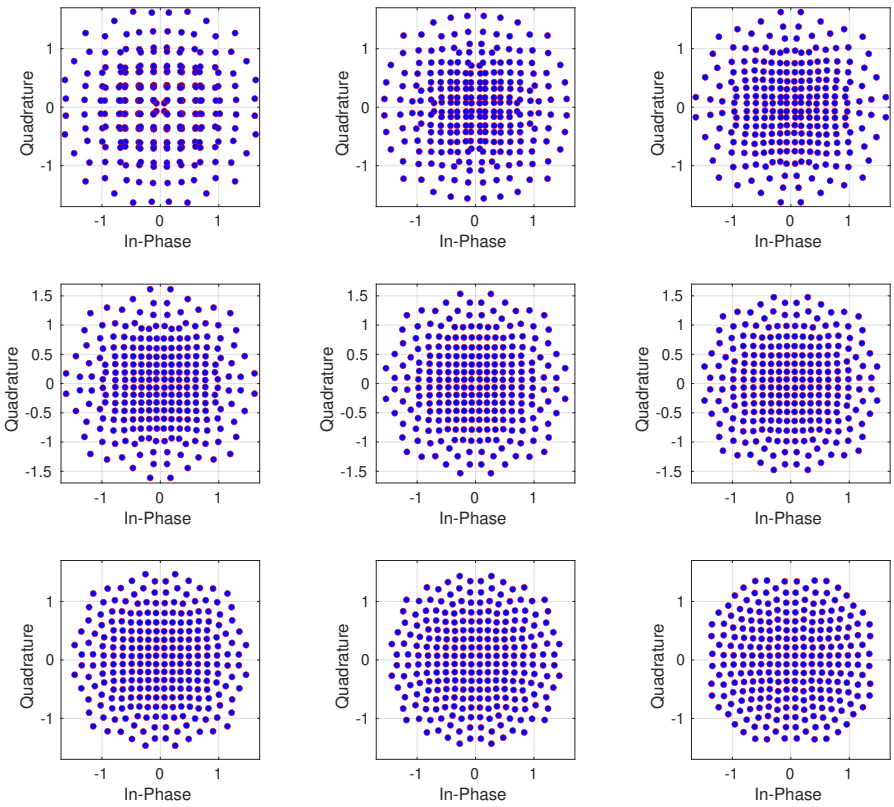

Figure 4.11: Optimized 256 2D–NUQAM for SNR values of 17, 18, 19, ..., 25 from top left to right.

Consequently, the complexity decreases to 70 parameters. Note that this will not fall into 62 parameters as 64 2D-NUQAM case, due to the standing of 8 constellation points on the $y = x$ or $y = -x$ line that do not have any mirror points inside the same quadrature.
Figure 4.11 shows the resulting symbol positions for SNR from 17 to 25 [dB]. It must be noted that depending on how the symmetry is chosen and which symbol positions are given to the optimizer as a parameter will result in different output shapes.
In the next section, there is a general conclusion about the value of possible gain using the optimized constellations. We will find 256 2D–NUQAM that delivers the maximum possible gain of 0.8 dB with $CR \approx 1/2$.

4.2.3 Conclusion of optimization gain

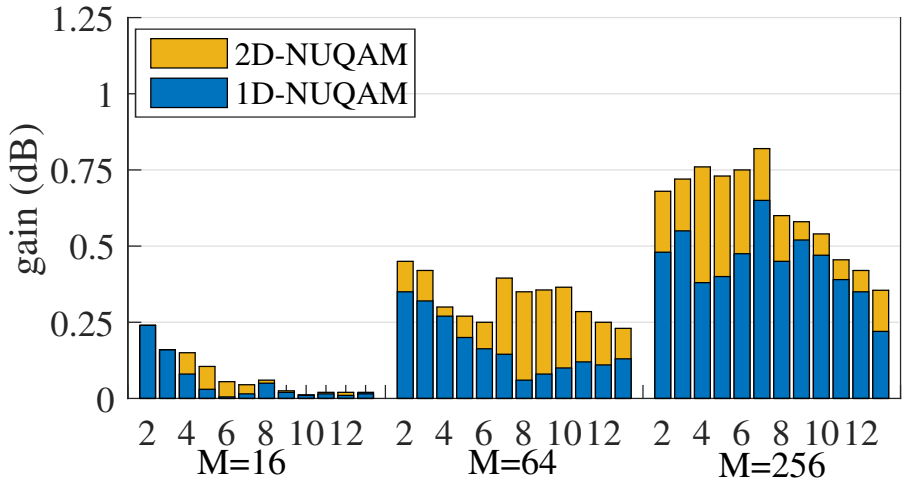

Figure 4.12: 1D and 2D NUQAM Performance gain under Rayleigh channel. CRs (x/15) from 2/15 to 13/15.

In the BICM capacity formula, which all the optimizations rely on that, the assumption is having a perfect channel coding unit. But in fact, we use different CRs. Remembering this, we should expect different gains for different CRs. In the figure 4.12, which is a modified version of figure available in [8], we see these variations. The values on this figure must be true also for our work since we both are using the same principle for optimization.
Based on the mentioned reference, in general, the highest gain is for medium Code Rates. As we stated earlier, because the gain is negligible when M = 16, we neither performed optimization nor discussed it.

4.2.4 Higher order NUQAM

Using the described principle, we can take an arbitrary M–ary QAM constellation and optimize it. As mentioned before, $M > 256$ is rarely used in the wireless industry. Especially nowadays that the trend is towards the higher frequencies and therefore the received power is very sensitive to the displacement of the mobile terminals [13].
Indeed, as M increases, considering the normalized power, the constellation symbols get close and closer to each other. It is true that if we increase M, each symbol will carry more bits, but at the end, the BER for a given SNR

is high due to the errors introduced by the mistaken demodulation. In order to compensate this loss, a better (lower) CR and a powerful FEC must be used.
In [19] the authors tried to optimize up to $M = 4096$ where the symbols merged. They used the term *Condensed* to describe this phenomenon. The reason for the condensation of symbols in lower SNRs is that they are going to preserve the Most significant bit (MSB) while eliminating the Least significant bit (LSB). With MSB, the position of a symbol can be decoded at the receiver, and as said before, the FEC can correct the errors. Therefore, we must expect that in sufficiently lower SNRs, 2^n–ary NUQAM constellations will be collapsed to an order of 2^{n-1} NUQAM.
Although using higher-order constellations increases the complexity of demodulation, the author in [19] states:

"*There is however a possible cause to like the idea of using ever-higher-order QAM constellations. Once we are improving the capacity at the margin, the capacity isn't increasing very much, but the increased constellation order means that the coded bit rate transmitted is increasing appreciably. In other words, the code rate of the FEC we have to use is becoming lower. Within reason, this may be a good thing, as it leaves something more in hand for dealing with selective channels.*
To put it very crudely, suppose a selective channel causes 1 bit in 4 to be erased 25 , then a code of rate 3/4 has nothing left to deal with noise (i.e. infinite SNR would be necessary). Only codes of lower rate than 3/4 would be usable in this example.
Suppose the intended operating point is 16.5 dB SNR, as just considered in the table of 6.6. The capacity that can be achieved is in the range 5.33 to 5.39 bit/symbol.
The implied code rate with 256-QAM (8 coded bit/symbol) is 5.33/8 = 0.67. With 1024-QAM (10 coded bit/symbol), the implied code rate is 5.39/10 = 0.539, a significant reduction."

Using the Soft decoding, for each bit, the LLR computation must be done. While the number of computations is M for uniform QAM and 1D–NUQAM, this value is doubling in 2D–NUQAM case (e.g. for 256 2D–NUQAM the complexity is 512). One possible solution to limit the LLR search area is to only select the area given by the Hard decoder. If the constellation is highly symmetrical like uniform M–ary QAMs, the search area defined by the Hard decoding is in order of $\log_2 M$. But, in the case of other constellations, specific methods need to be developed. While this document is being written, some of them emerged. For example in reference [8], *Quadrant Condensed*

Search Reduction (QCSR) is explained, and the author concluded a decrease in complexity "from 69% to 93%", while the loss comparing to Maximum-Likelihood (ML) is almost negligible. Further trials can be found in [3].

The final word in this chapter is that to choose the mode (non–uniform vs. uniform) and order of a constellation, all the associated factors which impact the loss/gain and implementation/adaptation complexity and cost must be evaluated. In this circumstance, the information of figure 4.12 can be helpful for making a decision.

Chapter 5

SDR and Performance evaluation

5.1 Introduction to SDR

Back in around 2010, when the new generation of processors released by manufacturers, there was a huge enhancement in the performance and functionality of processors. Year after year new processors are born with new architecture and instructions embedded in them and almost doubled in transistor number according to more's low while they are getting smaller and smaller in size. With current powerful computers and embedded systems, the vast majority of the signal processing can be handled [almost] in real-time inside the processor itself at the software level, and we do not need to have a dedicated separate piece of hardware to do such processing. Having an RF front end connected to our processors or some reconfigurable hardware like Field-programmable gate array (FPGA) is enough to prepare a fully operating radio communication system. Then the rest of the communication system units like [de]Interleaver, [de/en]coder, [de]mapper, [de]modulator, etc. can be implemented as software units running in our processors making a complete chain. The concept of the Software-defined radio (SDR) is actually an old one, but especially nowadays we have processing units in our hands to accomplish such tasks.
The importance of SDR is coming from the fact that we are capable of making a highly flexible communication system. We can adjust most of the parameters and switches between protocols by writing a new piece of code or just adjusting them. Moreover, if the system is open-source, we can share

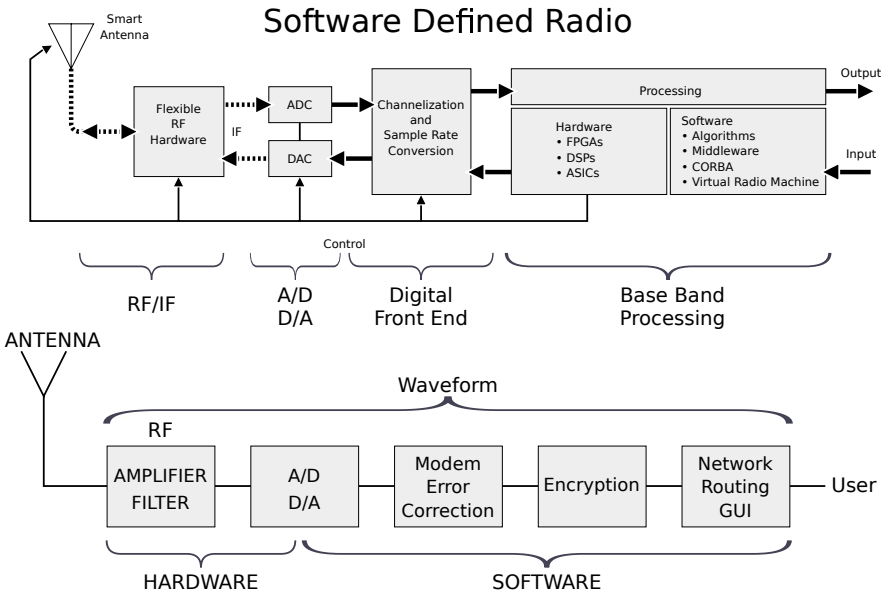

Figure 5.1: A graphical representation of SDR taken from Wikimedia.

either the binary or source code, which indeed is very meaningful these days and of course, useful. This was just a general high-level description of the idea behind the SDR. In the figure 5.1 a graphical representation of SDR is provided. So far, all the works done by the few published materials are in optimization using available tools like MATLAB or Wolfram Mathematica. The published papers and reports analyzed and discussed the performance using the data coming from the simulations in MATLAB or similar software.

In this work, we used SDR to implement what we designed and simulated before. Certainly, our focus is on implementing a mapper for new optimized NUQAM constellations and then having a setup to evaluate the performance in the real world.

5.2 System setup

In this thesis, *GNU Radio* [9] is used to build a realistic model of the REDS transmission chain as described before and depicted in the figure 2.8. Making the model more realistic introduces additional noise and losses so that the received SNR at the receiver will be shifted by some decibels.
The implementation consists of all the blocks that exist in DVB–T chain except that REDS substituted some of them that are mentioned in section 2.3.

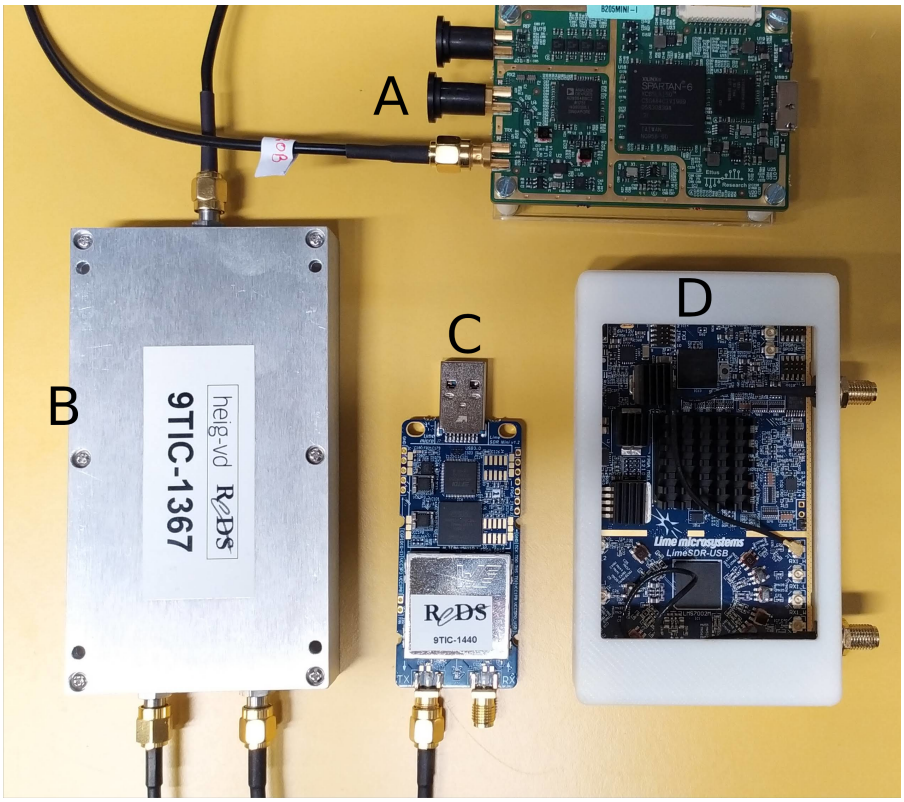

Figure 5.2: Test bed hardware. A: USRP board used as a transmitter. B: Signal combiner to add controlled noise to the signal. C: LimeSDR board used as receiver. D: LimeSDR board used as a noise generator.

For our aim, the transmission chain is adapted: the Mapper and Demapper blocks are redesigned to be able to apply the new non-uniform constellations and the existing chain is modified in order to pass some parameters to switch between various versions of the constellations. We used *liquid-dsp* [14], an open library written in C/C++, which can be interfaced with Gnu Radio in our mapper and demapper implementations.

Figure 5.2 shows the hardware used to complete the SDR chain and have a fully operational system. As can be seen in this figure, to have control on the noise level and avoid the impact of the environmental factors like multi-path fading, etc. we used a block of noise generator implemented in software and hardware to transmit and add this noise to the transmitting signal.

The latter figure 5.3 is a screenshot of the spectrum analyzer which shows the spectrum of the transmitting OFDM signal and added noise. This spectrum consists of 1705 sub-carriers, meaning that we have Fast Fourier

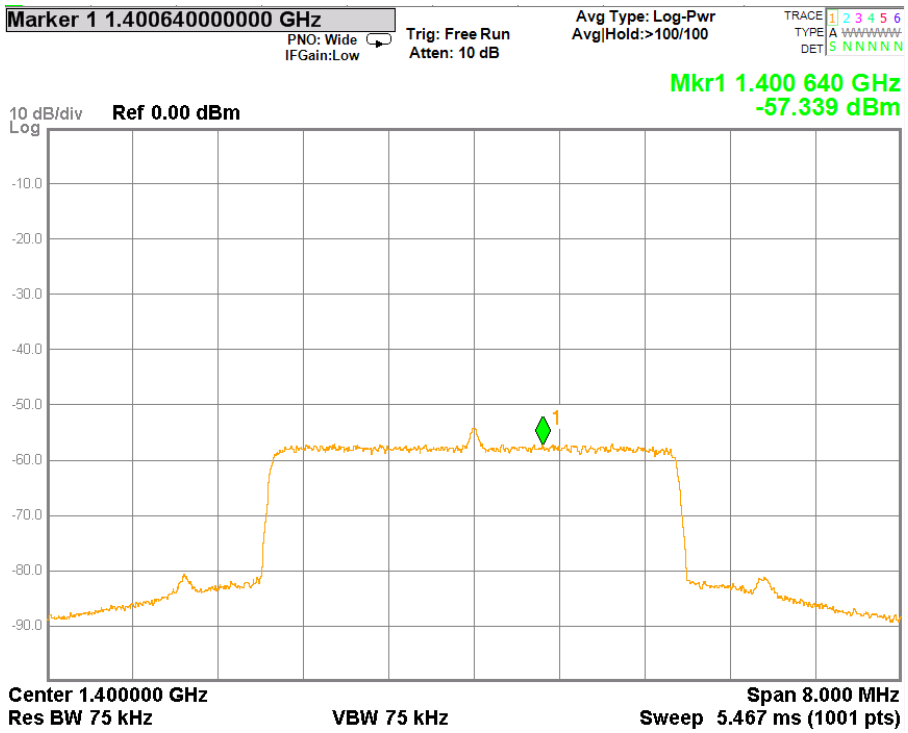

Figure 5.3: OFDM spectrum of the system as seen on spectrum analyzer.

transform (FFT) length of 2048 operating on 2K mode of DVB–T. Center frequency is 1.4 (GHz) and the bandwidth (BW) is set to 4 (MHz). Considering that in DVB–T standard, the sampling frequency is:

$$f_s = \frac{8}{7} \times BW_Hz \tag{5.1}$$

we get about 4.571 Mega samples.
The other important configuration parameters used in the test bed are as follows:

- Turbo Code block size = 576;
- Number of OFDM symbols per frame = 68;
- Guard Interval = 128;
- Constellation set = 64 QAM, 64 1D–NUQAM, 256 1D–NUQAM, 64 2D–NUQAM, 256 2D–NUQAM.

5.3 Data alignment

To have an accurate BER calculation, we need to have the input data and the received one to be precisely aligned, i.e. having the exact starting point. Misalignment happens because we can not turn the receiver on time to receive the data; As a result, we either have an unknown sequence of data recorded before beginning the useful information, or we started to record after transmission commences and have missed some portions of data. So the idea is to find the exact offset or address where the input and output data are getting aligned.
We can either process the input/output data directly, or we can inject the data after Interleaver (behind the turbo encoder) and collect it after turbo decoder (behind the deinterleaver).
For our goal, the cross-correlation method is employed to estimate the lag/delay between input and output. Besides, a direct pattern search using open–source tool *binwalk* is applied from the estimated offset by the first step, to ensure the files are aligned correctly to have reliable BER result.

Here we show an example of this approach. The two signals s_1 and s_2 (figure 5.4) represent our source and received files. Obviously, in our case s_2 is a delayed and noisy copy of s_1.
The cross-correlation of two jointly stationary random processes x_n and y_n where they assumed to be only a segment (N samples) of one realization of the infinite length random process is:

$$R_{x,y}(m) = \begin{cases} \sum_{n=0}^{N-m-1} x_{n+m} y_n^* & m \geq 0 \\ \\ R_{x,y}^*(-m) & m < 0 \end{cases} \tag{5.2}$$

and cross-correlation sequence is:

$$C(m) = R_{x,y}(m-n), m = 1,2,...,2N-1 \tag{5.3}$$

therefore, the delay is the index of the $C(m)$ where it has the maximum value. This is well illustrated in figure 5.5 where the lag between two signals is 127. This means that s_2 has a delay of 127 and we need to truncate the first 127 samples of it.
Finally in figure 5.6 after compensation of the delay, the two signals s_1 and s_2 are shown.

Note that if we consider the QEF criterion and make the alignment procedure easier, it would be better to generate a binary data file with enough

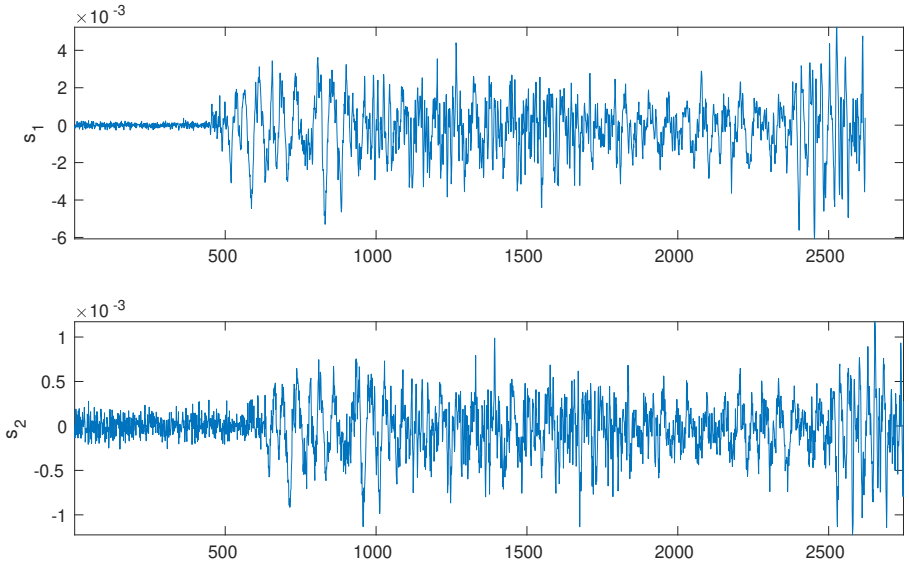

Figure 5.4: s_1 and s_2 signals.

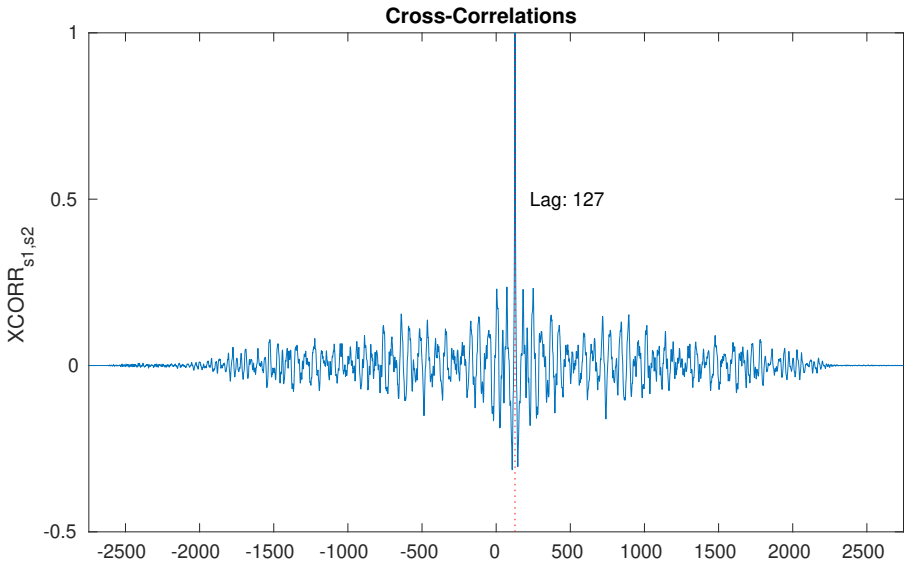

Figure 5.5: Maximum value of cross-correlation of s_1 and s_2 and corresponding index.

length and inject it into the system just before the turbo encoder and collect the output right after the turbo decoder. Since the Energy dispersal and RS decoder blocks are avoided in this method, it is vital to have a random sequence.

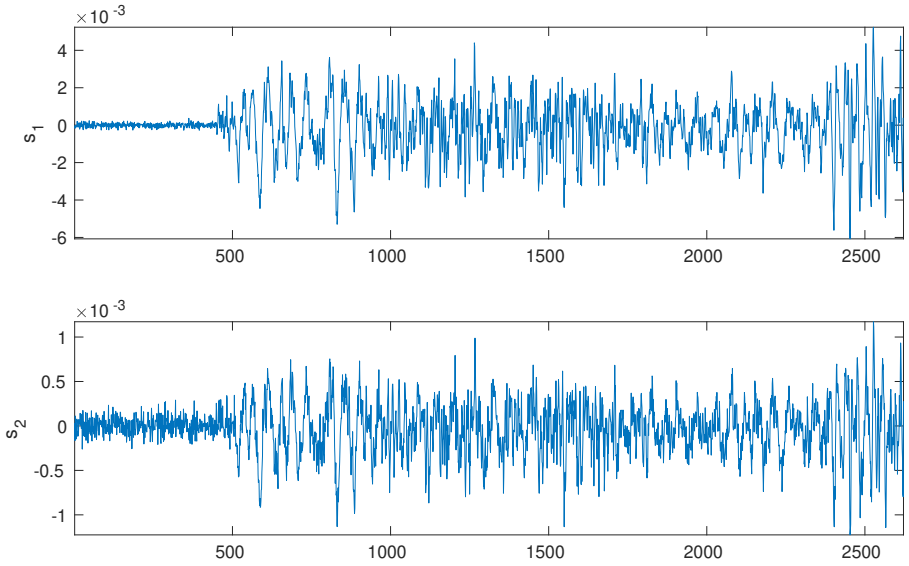

Figure 5.6: s_1 and s_2 are aligned.

5.4 BER calculation

5.4.1 Synchronization impact on SNR value

In MATLAB simulation, ideal conditions are assumed, i.e. ideal synchronization and ideal channel estimation. In reality, the receiver needs to determine the exact clock and frequency for sampling (Resampler) and then find the exact offset on the received OFDM frame where a new OFDM symbol is located. To do this various hierarchy of synchronization is done on the data with the aid of continual and scattered pilots, before passing it to OFDM demodulator and higher blocks. These blocks are shown in figure 5.7.
This process introduces a loss in the range of 1 to 5 [dB] in the real system performance. For this reason, in the real tests, it is not possible to reproduce exactly the performance simulation results, consequently, the measured signal and noise powers do not indicate the original SNR value in which the optimizations are done on constellations.
In this section, the transmission and noise power are measured separately before starting the transmission, then the two signals are fed into a signal combiner. We avoid using the antenna in our tests (instead SMA cables are used) to achieve more reliable outcomes. We reported the aforementioned powers instead of SNR.

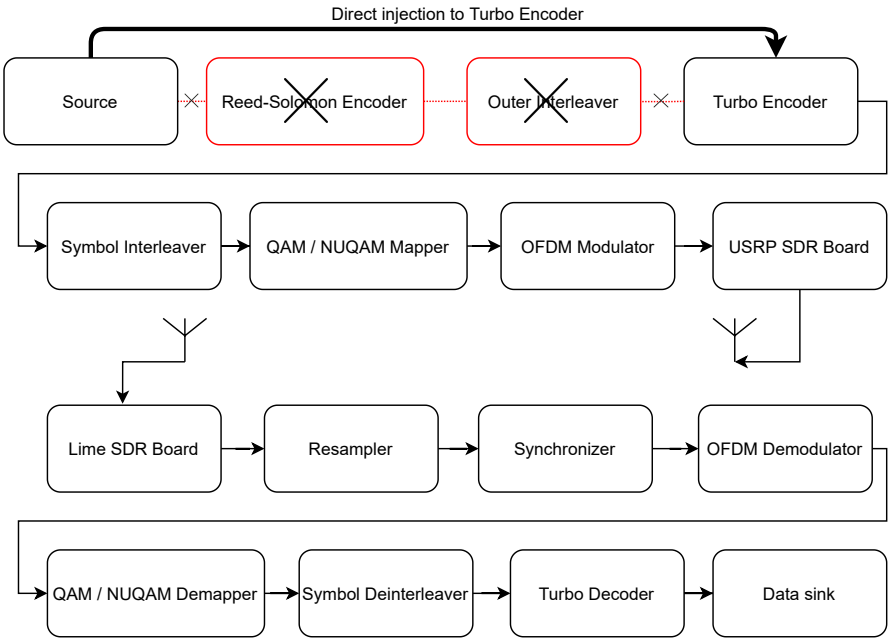

Figure 5.7: The model used to evaluate the performance of constellations.

5.4.2 Reed-Solomon impact on BER

Using the QEF criterion to evaluate the optimized constellations, it is required to count the BER at the input of the Reed-Solomon decoder at the receiver side. Since this coder works with 8-bit units to detect and correct the errors, counting the errors lacks enough accuracy to convert it to **bit** error rate, actually, that is more similar to Sequence Error rate (SER). In figure 5.7 the modified chain and location of input data injection and output collection is depicted. We used this model to calculate BER in our tests.

5.4.3 Error rate evaluation methods

Packet error rate and loss

Before we go to use the modified transmitter and receiver chain, we also wanted to use the original chain to show the performance of the system with the new constellation, despite that we already know this method is not flawless.
Fortunately, the Packet error rate is calculated by the implemented software in the runtime at each transmission interval. Here, the transmission interval is defined as the transmission of 10000 TS packets which each of which has

a length of 188 (bytes). In this thesis we are calling this *Instantaneous BER* since the value is multiplied by 8 to represent an approximate BER value, making it comparable with QEF. After 275 iterations (transmission of 4.136 megabits of data), the computed *Instantaneous BER* values are averaged and called BER.

Unlike the MATLAB simulations, in reality, if the transmission power is low or equivalently the noise level is high, there won't be any information about errors from the Reed-Solomon so the system will mark all the data in a packet as errors. So to make the performance analysis more reliable, we must avoid setting too low power values.
Furthermore, if the received SNR is high enough, errors occur rarely and so, there will be a very small number of times that we can see Instantaneous BER values to be smaller than QEF, as a result the participation of these errors in the averaged BER will be too low to appear in the result. Therefore, in these cases, to have an intuitive idea about the BER, counting the packet loss occurrence or equivalently when the *instantaneous BER* is bigger than QEF value could be an option.
Table 5.1 shows an example of the application of this method. This result is for 3 full transmissions of a 50 (MBytes) source stream file.
It compares 64 1D–NUQAM and uniform QAM; and verifies the superior performance of 64 1D–NUQAM over uniform QAM at received SNR of 15 [dB] and CR of 1/3, using REDS SDR transmission chain in GNU Radio.
In this table "# BER > QEF" counts the occurrence of BER values that are greater than QEF, and "# PACKET LOSS" indicates the corresponding TS packet loss occurrence during the test. Also, the "@SNR" denotes the optimized 64 1D–NUQAM constellation for that SNR, and "U" is the uniform QAM.
From the 3 mentioned performance factors in the table, it is clear that the optimized constellation for SNR closer to the working SNR point has better performance than the others. Here, optimized constellations for SNR of 14.8 and 15 are the best, while uniform QAM has the worst performance. As

64 1D–NUQAM	U	@14.8	@15	@15.2	@20
BER	6.34E-5	3.02E-5	3.15E-5	3.55E-5	4.2E-5
# BER > QEF	9.3	4.5	4.6	5.6	6
# PACKET LOSS	102	49.5	51.3	62.3	66

Table 5.1: Performance evaluation of 64 1D-NUQAM at $SNR = 15$.

explained in this section, this method is not accurate enough and even not fair enough to compare the two forms of constellation performances. For this reason, we performed this test just to provide an example and then moved towards the next method.

Bitwise error computation

First case: M = 64

In the BICM model, we assumed that the FEC is sufficiently powerful. We know that Reed-Solomon (RS) encoder and decoder blocks already exist in both REDS and DVB–T chain and it is necessary to keep these blocks. Removing them from the original transmission chain can decrease the overall performance of the system. But until the conditions for QAM and NUQAM constellations are equal, we can have an acceptable performance comparison. Since performing each test was time-consuming and we did not have enough time to do multiple tests to reproduce the figures and curves like those produced by the simulations in MATLAB (i.e. BER vs SNR), we decided to set the transmitting power and CR in the transmitter, then fix the gains in both sides and also in the noise generator. After this, we performed the tests for a sufficient duration, or equivalently, enough transferred data length inserting a new constellation each time. At the first attempt, we used this method to perform the previous test with the same parameters. Comparing the original and received files bit by bit after perfect alignment, results figure 5.8. Since we are reading the data as 8-bit unsigned integers, we can define byte error rate (ByteER), which indicates how many bytes are received wrong. This term is used just to have something similar to the previous test method. In this figure, BER and byte error rate curves are depicted for QAM and 64 1D–NUQAM constellations at TX power $\approx$ -87.2 [dBm] and Noise power $\approx$ -91.2 [dBm] in the AWGN channel. From the figure, it can be seen that both of the curves follow almost the same path. On the X-axis, the first element is uniform QAM, and the latter (@SNR) is the optimized constellation for a particular SNR value.

This figure confirms the better performance of 1D–NUQAM constellations in this SNR range comparing uniform QAM.

It is necessary to mention that the performance of NUQAM is very important in the waterfall region of the BER curves. According to [17] the region of the curve just before the sudden drop in performance is called the waterfall region of the error-rate curve. Indeed, despite the small performance gap between NUQAM and QAM in the waterfall region due to the steep slope of

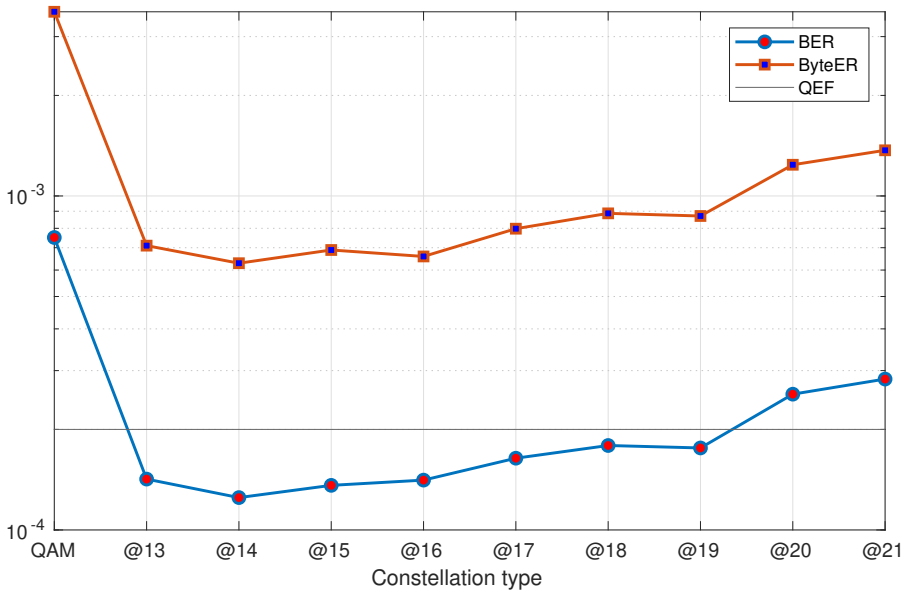

Figure 5.8: BER and Byte error rate of 64QAM and different types of 64 1D-NUQAM with CR=1/3, TX power ≈ -87.2 [dBm] and Noise power ≈ -91.2 [dBm] in the AWGN channel.

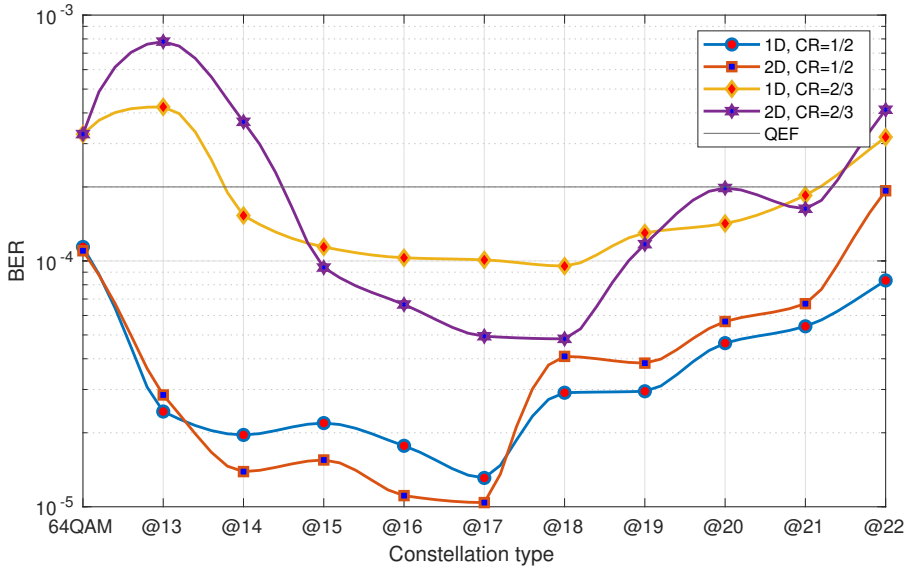

Figure 5.9: BER values of 64QAM and different types of 64 1D and 2D NUQAM: CR = 1/2, TX power ≈ -68 [dBm] and Noise power ≈ -85.5 [dBm]; CR = 2/3, TX power ≈ -65.5 [dBm] and Noise power ≈ -85.7 [dBm]. In AWGN channel.

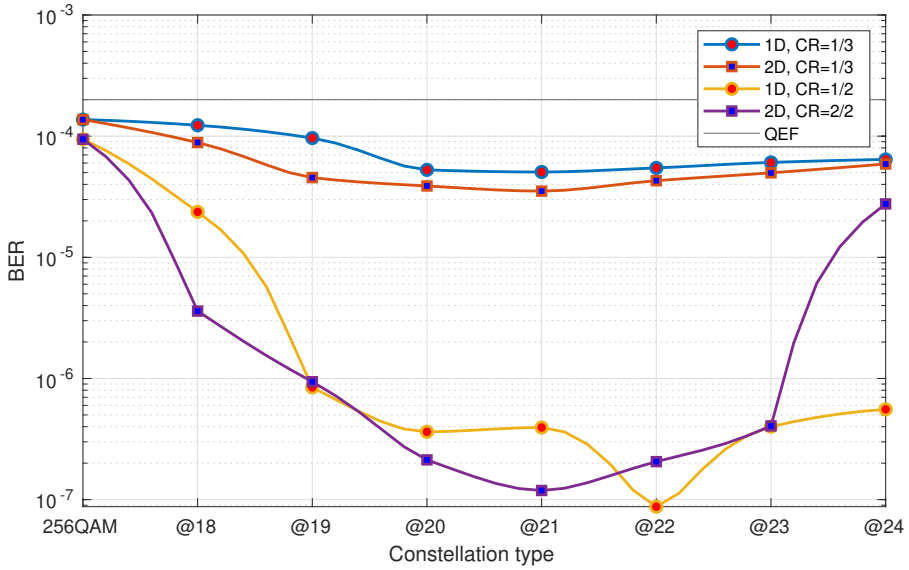

Figure 5.10: BER values of 256QAM and different types of 256 1D and 2D NUQAM: CR = 1/3, TX power ≈ -65.5 [dBm] and Noise power ≈ -85.7 [dBm; CR = 1/2, TX power ≈ -58 [dBm] and Noise power ≈ -89 [dBm]. In AWGN channel.

the BER curve, if NUQAM is used, then the receiver can demodulate and decode all the data successfully, while this is not true using uniform QAM.

Figure 5.9 shows the BER value for each optimized 1D and 2D constellation with M = 64, for CR of 1/2 and 2/3. The complete information is written in the figure description. Note that the first case in the X-axis is the BER value corresponding to uniform 64QAM. Besides, we smoothed the curves to have a better illustration.
In both cases, the optimized constellations in SNR 16 and 17 have the best BER values. From the curves, it seems the 2D NUQAM constellations are more sensitive to the operation point, as we see some of them (usually) performing better than other 2D and 1D versions, but always have better performance than the uniform version.

Second case: M = 256

The BER measurements for higher orders were not easy and in each iteration, we got scattered values. This shows their sensitivity to the noise. So, through several trials, we adjusted the transmission and noise power so that the BER never went above the QEF line and stays near that point. After fixing the power, we averaged the results of various trials in each point and

could draw the resulting figure 5.10.
We can see a general trend in all these figures: beginning from uniform QAM, the number of errors with optimized constellations on the SNR point that they were optimized in, decreases. Up to a point this continues to reach a minimum which is the point that the best performing NUQAM is located. After that, as we must expect, the error begins to grow and continues to converge to a value in which the optimized constellation symbols are apart from each other, keeping the same distance, resembling the uniform QAM shape. We observed this in all the curves we have.

Chapter 6

Conclusions and Future work

In this thesis, we had a short introduction to the BICM systems, trying to make them perform better. Then we discussed the REDS transmission chain in which the re-engineered transmitter tries to transfer more bits in a time unit while maintaining the error level acceptable without a huge power increase.
This work is essential these days; because we are going to generate more and more data every day. Especially in the video broadcasting industry, by emerging of the larger TV screens, the human vision wants to observe a clear picture which means the resolution must be increased and consequently the bit rate.
In this regard, we used the BICM capacity as a key and a straightforward method for optimizing the constellation in the modulation block of the chain. Optimizing leads to close the gap between the uniform M–ary QAM constellations and the upper capacity bound, which is known as Shannon limit. After discussing the NM algorithm, we started the optimization process. Given a set of initial symbol positions corresponding to a constellation of order M, the output of the process was a set of optimum positions of the symbols where BICM capacity reached its maxima. As the resulting constellations depend on the SNR where the optimization is performed, at lower SNRs, symbols begin to merge and become condensed, making condensed constellations concepts. This concept was investigated on the other references and we summarized it too. In this work, instead, we focused on the working point power levels of the transmission system, which is not too low to have such

constellations in use. The performance of these constellations is first evaluated in the MATLAB, close to the working point of DVB–T systems called QEF. We found this point interesting because for BER values below this, the stream can be demodulated and its errors can be corrected by having a clear smooth video playback.
As the title indicates, the most important aspect of this work is the study and evaluation of the proposed constellations in a real system. For this, we used the REDS chain to test them, and indeed the superior performance of the new constellations is proved. Setting the transmission power level system near the location where the QEF criterion is fulfilled had an important outcome: using the optimized constellation the system can operate normally and stay more stable. Especially in the waterfall region of the BER curves where the system is prone to errors due to various types of noise by small variations in received power levels. this means that BER can stay further below the QEF criteria.
However, one issue in the application of these constellations is the complexity increase in the demodulation block at the receiver. This can not be a problem anymore with the new low-power high-performance hardware since the new methods were developed decreasing the complexity dramatically with a negligible performance loss.
The actual challenge remains to choose the right constellation for the system to operate. There are many constellations, each having the best performance in a specific SNR. Considering that the receiver stations are located at different distances from the transmitter, thus experiencing a different level of power and noise, the results based on the experiments in the last section of this document show that a wide range of the optimized constellations at least have equal and in general better performance than the uniform QAM.
To benefit from various types of these optimized constellations and have a robust broadcasting system, an adaptive transmitter and receiver can be designed. In this case, signaling can be used to inform the receiver about new parameters of the new constellations.
Finally, looking at the image that this work gives, as exists in all communication systems, there is also a trade-off between implementation cost, complexity, power consumption, and the gain which is discussed in chapter 4. At most, the 0.8 [dB] gain in terms of power can be achieved, where M is 256 and CR approximately 1/2 using 2D optimized constellation, while this is 0.65 in the case where M is 64 and again CR 1/2. Therefore this needs to be considered in the design of a communication system.

The optimized constellations can be used in every transmission system

that follows the BICM scheme. Also, the same method that is used to optimize square-shaped constellation applies to the other constellations like APSK to find the optimum radius and location of the symbols. Looking far from constellations, there are still several blocks in the transmission chain that each of them can be optimized further. But also there are other opportunities for further work in the other areas related to the gain in terms of bit rate in a video broadcasting system. One of the most interesting elements is source encoders. We see significant progress in video encoding in the past 10 years and it is proceeding. The recent research led to introduce the latest video codec: Versatile Video Coding (VVC) [4] and of course, fast implementations of this new technology is very effective to satisfy the need for high bit rates.

Bibliography

[1] F. Abdelkefi, *To2020 project technical report*, REDS Institute, Haute Ecole d'Ingénierie et de Gestion du Canton de Vaud, (2018).

[2] A. Alvarado, E. Agrell, and A. Svensson, *On the capacity of bicm with qam constellations*, in Proceedings of the 2009 International Conference on Wireless Communications and Mobile Computing: Connecting the World Wirelessly, IWCMC '09, New York, NY, USA, 2009, Association for Computing Machinery, p. 573–579.

[3] J. Barrueco Gutierrez, J. Montalban, P. Angueira, C. Abdel Nour, and C. Douillard, *Low Complexity Adaptive Demapper for 2-D Non-Uniform Constellations*, IEEE Transactions on Broadcasting, 65 (2019), pp. 10–19.

[4] B. Bross, J. Chen, J. R. Ohm, G. J. Sullivan, and Y. K. Wang, *Developments in international video coding standardization after avc, with an overview of versatile video coding (vvc)*, Proceedings of the IEEE, (2021), pp. 1–31.

[5] G. Caire, G. Taricco, and E. Biglieri, *Bit-interleaved coded modulation*, IEEE Transactions on Information Theory, 44 (1998), pp. 927–946.

[6] O. Edfors, M. Sandell, J. van de Beek, D. Landström, and F. Sjöberg, *An introduction to orthogonal frequency-division multiplexing*, Luleå tekniska universitet, 1997.

[7] European Telecommunications Standards Institute, *Digital Video Broadcasting (DVB); Framing structure, channel coding and modulation for digital terrestrial television*, etsi en 300 744 v1.6.1 ed., 2009.

[8] M. Fuentes Muela, *Non-Uniform Constellations for Next-Generation Digital Terrestrial Broadcast Systems*, PhD thesis, Departamento de Comunicaciones Universitat Politècnica de València, 2017.

[9] GnuRadio, *Gnuradio*. `https://www.gnuradio.org`.

[10] M. Inc, *Digital modulation*. `https://www.mathworks.com/help/`

comm/ug/digital-modulation.html#brc6ymu.

[11] F. Kayhan and G. Montorsi, *Constellation design for memoryless phase noise channels*, IEEE Transactions on Wireless Communications, 13 (2014), pp. 2874–2883.

[12] J. Lagarias, J. Reeds, M. Wright, and P. Wright, *Convergence properties of the nelder-mead simplex method in low dimensions*, SIAM Journal on Optimization, 9 (1998), pp. 112–147. Copyright: Copyright 2017 Elsevier B.V., All rights reserved.

[13] J. Lee, M.-D. Kim, J.-J. Park, and Y. J. Chong, *Field-measurement-based received power analysis for directional beamforming millimeter-wave systems: Effects of beamwidth and beam misalignment*, ETRI Journal, 40 (2018), pp. 26–38.

[14] liquid dsp, *liquid-dsp*. https://github.com/jgaeddert/liquid-dsp.

[15] H. Nyquist, *Certain topics in telegraph transmission theory*, Transactions of the American Institute of Electrical Engineers, 47 (1928), pp. 617–644.

[16] M. Rupp, S. Schwarz, and M. Taranetz, *The Vienna LTE-Advanced Simulators: Up and Downlink, Link and System Level Simulation*, Springer Publishing Company, Incorporated, 1st ed., 2016.

[17] W. Ryan and S. Lin, *Low-Density Parity-Check Codes*, Cambridge University Press, 2009, p. 201–256.

[18] F. Steiner and G. Böcherer, *Comparison of geometric and probabilistic shaping with application to ATSC 3.0*, CoRR, abs/1608.00474 (2016).

[19] J. Stott, *Cm and bicm limits for rectangular constellations*, BBC R&D White Paper WHP, 257 (2013).

[20] A. J. Viterbi, *An intuitive justification and a simplified implementation of the map decoder for convolutional codes*, IEEE Journal on Selected Areas in Communications, 16 (1998), pp. 260–264.

[21] Wikimedia, *Nelder-mead optimisation method in a one-dimensional space*. https://commons.wikimedia.org/wiki/File:Algorithme_Nelder_Mead_1D.svg.

[22] E. Zehavi, *8-psk trellis codes for a rayleigh channel*, IEEE Transactions on Communications, 40 (1992), pp. 873–884.